# Characteristic Evolution and Matching

Jeffrey Winicour
Max-Planck-Institut für Gravitationsphysik, Albert-Einstein-Institut,
14476 Golm, Germany
and
Department of Physics and Astronomy,
University of Pittsburgh, Pittsburgh, PA 15260, USA
email: jeff@einstein.phyast.pitt.edu

*Published on 20 March 2001*
*www.livingreviews.org/Articles/Volume4/2001-3winicour*
*Living Reviews in Relativity*
*Published by the Max Planck Institute for Gravitational Physics*
*Albert Einstein Institute, Germany*

**Abstract**

I review the development of numerical evolution codes for general relativity based upon the characteristic initial value problem. Progress is traced from the early stage of 1D feasibility studies to current 3D codes that simulate binary black holes. A prime application of characteristic evolution is Cauchy-characteristic matching, which is also reviewed.

# Article Amendments

On author request a *Living Reviews* article can be amended to include errata and small additions to ensure that the most accurate and up-to-date information possible is provided. For detailed documentation of amendments, please go to the article's online version at

`http://www.livingreviews.org/Articles/Volume4/2001-3winicour/.`

Owing to the fact that a *Living Reviews* article can evolve over time, we recommend to cite the article as follows:

Winicour, J.,
"Characteristic Evolution and Matching",
*Living Rev. Relativity*, **4**, (2001), 3. [Online Article]: cited on <date>,
http://www.livingreviews.org/Articles/Volume4/2001-3winicour/.

The date in 'cited on <date>' then uniquely identifies the version of the article you are referring to.

# Contents

# 1 Introduction

It is my pleasure to review progress in numerical relativity based upon characteristic evolution. In the spirit of Living Reviews, I invite my colleagues to continue to send me contributions and comments at jeff@einstein.phyast.pitt.edu.

We have entered an era in which Einstein's equations can effectively be considered solved at the local level. Several groups, as reported here and in other Living Reviews, have developed 3D codes which are stable and accurate in some sufficiently local setting. Global solutions are another matter. In particular, there is no single code in existence today which purports to be capable of computing the waveform of gravitational radiation emanating from the inspiral and merger of two black holes, the premier problem in classical relativity. Just as several coordinate patches are necessary to describe a spacetime with nontrivial topology, the most effective attack on the binary black hole problem is likely to involve patching together regions of spacetime handled by different codes.

Much work in numerical relativity is based upon the Cauchy $\{3 + 1\}$ formalism [156], with the gravitational radiation extracted by perturbative Cauchy methods which introduce an artificial Schwarzschild background [1, 3, 2, 142]. These wave extraction methods have not been tested in a nonlinear 3D setting. A different approach which is specifically tailored to study radiation is based upon the characteristic initial value problem. In the 1960's, Bondi [34, 35] and Penrose [111] pioneered the use of null hypersurfaces to describe gravitational waves. This new approach has flourished in general relativity. It yields the standard description of the "plus" and "cross" polarization modes of gravitational radiation in terms of the real and imaginary parts of the Bondi news function at future null infinity $\mathcal{I}^+$.

From a computational standpoint, the major drawback of the characteristic approach arises from the formation of caustics in the light rays generating the null hypersurfaces. In the most ambitious scheme proposed at the theoretical level such caustics would be treated "head-on" as part of the dynamical problem [136]. This is a profoundly attractive idea. Only a few structural stable caustics can arise in numerical evolution, and their geometrical properties are well enough understood to model their singular behavior numerically [62]. However, a computational implementation of this approach has not yet been achieved. It is a great idea that is perhaps ahead of its time.

In the typical setting for the characteristic initial value problem, the domain of dependence of a single nonsingular null hypersurface is empty. In order to obtain a nontrivial evolution problem, the null hypersurface must either be completed to a caustic-crossover region where it pinches off, or an additional boundary must be introduced. So far, the only caustics that have been successfully evolved numerically in general relativity are pure point caustics (the complete null cone problem). When spherical symmetry is not present, it turns out that the stability conditions near the vertex of a light cone place a strong restriction on the allowed time step [91]. Point caustics in general relativity have been successfully handled this way for axisymmetric spacetimes [74], but

the computational demands for 3D evolution would be prohibitive using current generation supercomputers. This is unfortunate because, away from the caustics, the characteristic evolution offers myriad computational and geometrical advantages.

As a result, at least in the near future, the computational application of characteristic evolution is likely to be restricted to some mixed form, in which data is prescribed on a non-singular but incomplete initial null hypersurface N and on a second boundary hypersurface B, which together with the initial null hypersurface determine a nontrivial domain of dependence. This second hypersurface may itself be either (i) null, (ii) timelike or (iii) spacelike. These possibilities give rise to (i) the double null problem, (ii) the nullcone-worldtube problem or (iii) the Cauchy-characteristic matching (CCM) problem, in which the Cauchy and characteristic evolutions are matched transparently across a worldtube W, as schematically depicted in Fig. 1.

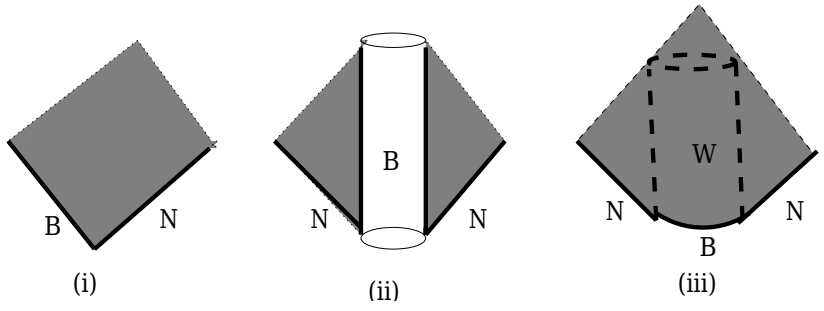


Figure 1: *The three applications of characteristic evolution with data given on an initial null hypersurface N and boundary B. The shaded regions indicate the corresponding domains of dependence.*

In CCM, it is possible to choose the matching interface between the Cauchy and characteristic regions to be a null hypersurface, but it is more practical to match across a timelike worldtube. CCM combines the advantages of characteristic evolution in treating the outer radiation zone in spherical coordinates which are naturally adapted to the topology of the worldtube with the advantages of Cauchy evolution in Cartesian coordinates in the region where spherical coordinates would break down.

In this review, we trace the development of characteristic algorithms from model 1D problems to a 3D code designed to calculate the waveform emitted in the merger to ringdown phase of a binary black hole. And we trace the development of CCM from early feasibility studies through current attempts to treat the binary black hole problem.

There have been several notable developments since my last review. Most important for future progress has been the award of three new doctorates, with theses based upon characteristic evolution codes: Denis Pollney [115] at the the University of Southampton, Luis Lehner [97] and Bela Szilágyi [137] at the University of Pittsburgh. Lehner received the Nicholas Metropolis award of

the American Physical Society for his thesis research, recognizing characteristic evolution as an important computational technique. In the area of scientific application, light cone evolution codes for hydrodynamics have been used to study astrophysical processes. In addition, a 3D characteristic vacuum code developed at the University of Canberra has been successfully applied to the scattering of waves off a Schwarzschild black hole (see Sec. 3.5) and the Pittsburgh 3D code is being applied to obtain the postmerger to ringdown waveform from binary black holes (see Sec. 3.6). Simulations from these studies can be viewed at the Canberra [149] and Pittsburgh [150] web sites.

## 2 The Characteristic Initial Value Problem

Characteristics have traditionally played an important role in the analysis of hyperbolic partial differential equations. However, the use of characteristic hypersurfaces to supply the foliation underlying an evolution scheme has been mainly restricted to relativity. This is perhaps natural because in curved spacetime there is no longer a preferred Cauchy foliation provided by the Euclidean 3-spaces allowed in Galilean or special relativity. The method of shooting along characteristics is a standard technique in many areas of computational physics, but evolution based upon characteristic hypersurfaces is quite uniquely limited to relativity.

Bondi's initial use of null coordinates to describe radiation fields [34] was followed by a rapid development of other null formalisms. These were distinguished either as metric based approaches, as developed for axisymmetry by Bondi, Metzner and van den Burg [35] and generalized by Sachs [122], or as null tetrad approaches in which the Bianchi identities appear as part of the set of equations, as developed by Newman and Penrose [106].

At the outset, null formalisms were applied to construct asymptotic solutions at null infinity by means of $1/r$ expansions. Soon afterwards, Penrose devised the conformal compactification of null infinity $\mathcal{I}$ ("scri"), thereby reducing to geometry the asymptotic description of the physical properties of the radiation zone, most notably the Bondi mass and news function [111]. The characteristic initial value problem rapidly became an important tool for the clarification of fundamental conceptual issues regarding gravitational radiation and its energy content. It laid bare and geometricized the gravitational far field.

The initial focus on asymptotic solutions clarified the kinematic properties of radiation fields but could not supply the waveform from a specific source. It was soon realized that instead of carrying out a $1/r$ expansion, one could reformulate the approach in terms of the integration of ordinary differential equations along the characteristics (null rays) [139]. The integration constants supplied on some inner boundary then determined the specific waveforms obtained at infinity. In the double-null initial value problem of Sachs [123], the integration constants are supplied at the intersection of outgoing and ingoing null hypersurfaces. In the worldtube-nullcone formalism, the sources were represented by integration constants on the worldtube [139]. These early formalisms have gone through much subsequent revamping. Some have been reformulated to fit the changing styles of modern differential geometry. Some have been reformulated in preparation for implementation as computational algorithms. See the articles in [50] for a representative sample of formalisms. Rather than including a review of the extensive literature on characteristic formalisms in general relativity, I concentrate here on those approaches which have been implemented as computational evolution schemes. The topic of well-posedness of the underlying boundary value problems, which has obvious relevance to the success of numerical simulations, is treated in a separate Living Review on Local and Global Existence Theorems by A. Rendall [119].

All characteristic evolution schemes share the same skeletal form. The fun-

damental ingredient is a foliation by null hypersurfaces $u$ = const. which are generated by a two-dimensional set of null rays, labeled by coordinates $x^A$, with a coordinate $\lambda$ varying along the rays. In $(u, \lambda, x^A)$ null coordinates, the main set of Einstein equations take the schematic form

$$F_{,\lambda} = H_F[F, G] \tag{1}$$

and

$$G_{,u\lambda} = H_G[F, G, G_{,u}]. \tag{2}$$

Here $F$ represents a set of hypersurface variables, $G$ a set of evolution variables, and $H_F$ and $H_G$ are nonlinear hypersurface operators, i.e. they operate locally on the values of $F$, $G$ and $G_{,u}$ intrinsic to a single null hypersurface. In addition to these main equations, there is a subset of four Einstein equations which are satisfied by virtue of the Bianchi identities, provided that they are satisfied on a hypersurface transverse to the characteristics. These equations have the physical interpretation as conservation laws. Mathematically they are analogous to the constraint equations of the canonical formalism. But they are not elliptic, since they are imposed upon null or timelike hypersurfaces, rather than spacelike Cauchy hypersurfaces.

# 3 Characteristic Evolution Codes

Computational implementation of characteristic evolution may be based upon different versions of the formalism (i.e. metric or tetrad) and different versions of the initial value problem (i.e. double null or worldtube-nullcone). The performance and computational requirements of the resulting evolution codes can vary drastically. However, most characteristic evolution codes share certain common advantages:

1. There are no elliptic constraint equations. This eliminates the need for time consuming iterative methods to enforce constraints.

2. No second time derivatives appear so that the number of basic variables is at least half the number for the corresponding version of the Cauchy problem.

3. The main Einstein equations form a system of coupled ordinary differential equations with respect to the parameter $\lambda$ varying along the characteristics. This allows construction of an evolution algorithm in terms of a simple march along the characteristics.

4. In problems with isolated sources, the radiation zone can be compactified into a finite grid boundary using Penrose's conformal technique. Because the Penrose boundary is a null hypersurface, no extraneous outgoing radiation condition or other artificial boundary condition is required.

5. The grid domain is exactly the region in which waves propagate, which is ideally efficient for radiation studies. Since each null hypersurface of the foliation extends to infinity, the radiation is calculated immediately (in retarded time).

6. In black hole spacetimes, a large redshift at null infinity relative to internal sources is an indication of the formation of an event horizon and can be used to limit the evolution to the exterior region of spacetime.

Characteristic schemes also share as a common disadvantage the necessity either to deal with caustics or to avoid them altogether. The scheme to tackle the caustics head on by including their development as part of the evolution is perhaps a great idea still ahead of its time but one that should not be forgotten. There are only a handful of structurally stable caustics, and they have well known algebraic properties. This makes it possible to model their singular structure in terms of Padé approximants. The structural stability of the singularities should in principle make this possible, and algorithms to evolve the elementary caustics have been proposed [47, 134]. In the axisymmetric case, cusps and folds are the only stable caustics, and they have already been identified in the horizon formation occurring in simulations of head-on collisions of black holes and in the temporarily toroidal horizons occurring in collapse of rotating matter [104, 127]. In a generic binary black hole horizon, where axisymmetry is broken, there is a

closed curve of cusps which bounds the two-dimensional region on the horizon where the black holes initially form and merge [100, 89].

## 3.1 {1 + 1}-Dimensional Codes

It is often said that the solution of the general ordinary differential equation is essentially known, in light of the success of computational algorithms and present day computing power. Perhaps this is an overstatement because investigating singular behavior is still an art. But, in the same vein, it is fair to say that the general system of hyperbolic partial differential equations in one spatial dimension is a solved problem. At least, it seems to be true in general relativity.

One of the earliest characteristic evolution codes, constructed by Corkill and Stewart [47, 133], treated spacetimes with two Killing vectors using a grid based upon double null coordinates, with the null hypersurfaces intersecting in the surfaces spanned by the Killing vectors. They simulated colliding plane waves and evolved the Khan-Penrose [96] collision of impulsive ($\delta$-function curvature) plane waves to within a few numerical zones from the final singularity, with extremely close agreement with the analytic results. Their simulations of collisions with more general waveforms, for which exact solutions are not known, provided input to the understanding of singularity formation which was unforseen in the analytic treatments of this problem.

Many {1 + 1}-dimensional characteristic codes have been developed for spherically symmetric systems. Here matter must be included in order to make the system non-Schwarzschild. Initially the characteristic evolution of matter was restricted to simple cases, such as massless Klein-Gordon fields, which allowed simulation of gravitational collapse and radiation effects in the simple context of spherical symmetry. Now, characteristic evolution of matter is progressing to more complicated systems. Its application to hydrodynamics, which is beginning to make significant contributions to general relativistic astrophysics, is reviewed in Sec. 5.

The synergy between analytic and computational approaches has already led to dramatic results in the massless Klein-Gordon case. On the analytic side, working in a characteristic initial value formulation based upon outgoing null cones, Christodoulou made a penetrating study of the existence and uniqueness of solutions to this problem [41, 40, 43, 42]. He showed that weak initial data evolve to Minkowski space asymptotically in time, but that sufficiently strong data form a horizon, with nonzero Bondi mass. In the latter case, he showed that the geometry is asymptotically Schwarzschild in the approach to $I^+$ (future time infinity) from outside the horizon, thus establishing a rigorous version of the no-hair theorem. What this analytic tour-de-force did not reveal was the remarkable critical behavior in the transition between these two regimes, which was discovered by Choptuik [38, 39] by computational simulation based upon Cauchy evolution. This phenomena has now been understood in terms of the methods of renormalization group theory and intermediate asymptotics, and has spawned a new subfield in general relativity, which is covered in a Living

Review on Critical Phenomena in Gravitational Collapse by C. Gundlach [79].

The characteristic evolution algorithm for the spherically symmetric Einstein-Klein-Gordon problem provides a simple illustration of the techniques used in the general case. It centers about the evolution scheme for the scalar field, which constitutes the only dynamical field. Given the scalar field, all gravitational quantities can be determined by integration along the characteristics of the null foliation. This is a coupled problem, since the scalar wave equation involves the curved space metric. It illustrates how null algorithms lead to a hierarchy of equations which can be integrated along the characteristics to effectively decouple the hypersurface and dynamical variables.

In a Bondi coordinate system based upon outgoing null hypersurfaces $u =$ const. and a surface area coordinate $r$, the metric is

$$ds^2 = -e^{2\beta} du \left( \frac{V}{r} du + 2dr \right) + r^2 (d\theta^2 + \sin^2 \theta d\phi^2). \tag{3}$$

Smoothness at $r = 0$ allows the coordinate conditions

$$V(u, r) = r + O(r^3) \quad \text{and} \quad \beta(u, r) = O(r^2). \tag{4}$$

The field equations consist of the wave equation $\Box \Phi = 0$ for the scalar field and two hypersurface equations for the metric functions:

$$\beta_{,r} = 2\pi r (\Phi_{,r})^2, \tag{5}$$

$$V_{,r} = e^{2\beta}. \tag{6}$$

The wave equation can be expressed in the form

$$\Box^{(2)} g - \left( \frac{V}{r} \right)_{,r} \frac{e^{-2\beta} g}{r} = 0, \tag{7}$$

where $g = r\Phi$ and $\Box^{(2)}$ is the D'Alembertian associated with the two-dimensional submanifold spanned by the ingoing and outgoing null geodesics. Initial null data for evolution consists of $\Phi(u_0, r)$ at initial retarded time $u_0$.

Because any two-dimensional geometry is conformally flat, the surface integral of $\Box^{(2)} g$ over a null parallelogram $\Sigma$ gives exactly the same result as in a flat 2-space, and leads to an integral identity upon which a simple evolution algorithm can be based [76]. Let the vertices of the null parallelogram be labeled by $N$, $E$, $S$ and $W$ corresponding, respectively, to their relative locations North, East, South and West in the 2-space, as shown in Fig. 2. Upon integration of (7), curvature introduces an area integral correction to the flat space null parallelogram relation between the values of $g$ at the vertices:

$$g_N - g_W - g_E + g_S = -\frac{1}{2} \int_\Sigma du dr \left( \frac{V}{r} \right)_{,r} \frac{g}{r}. \tag{8}$$

This identity, in one form or another, lies behind all of the null evolution algorithms that have been applied to this system. The prime distinction between

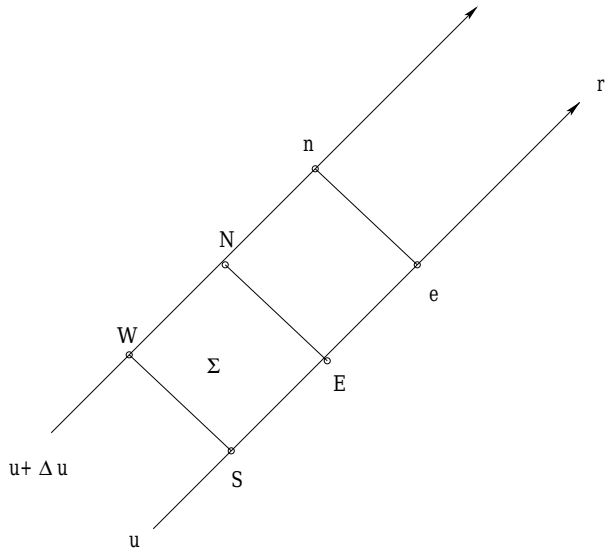


Figure 2: *The null parallelogram. After computing the field at point $N$, the algorithm marches the computation to $\mathcal{I}^+$ by shifting the corners by $N \to n$, $E \to e$, $S \to E$, $W \to N$.*

the different algorithms is whether they are based upon double null coordinates or Bondi coordinates as in Eq. (3). When a double null coordinate system is adopted, the points $N$, $E$, $S$ and $W$ can be located in each computational cell at grid points, so that evaluation of the left hand side of Eq. (8) requires no interpolation. As a result, in flat space, where the right hand side of Eq. (8) vanishes, it is possible to formulate an exact evolution algorithm. In curved space, of course, there is a truncation error arising from the approximation of the integral by evaluating the integrand at the center of $\Sigma$.

The identity (8) gives rise to the following explicit marching algorithm, indicated in Fig. 2. Let the null parallelogram lie at some fixed $\theta$ and $\phi$ and span adjacent retarded time levels $u_0$ and $u_0 + \Delta u$. Imagine for now that the points $N$, $E$, $S$ and $W$ lie on the spatial grid, with $r_N - r_W = r_E - r_S = \Delta r$. If $g$ has been determined on the initial cone $u_0$, which contains the points $E$ and $S$, and radially outward from the origin to the point $W$ on the next cone $u_0 + \Delta u$, then Eq. (8) determines $g$ at the next radial grid point $N$ in terms of an integral over $\Sigma$. The integrand can be approximated to second order, i.e. to $O(\Delta r \Delta u)$, by evaluating it at the center of $\Sigma$. To this same accuracy, the value of $g$ at the center equals its average between the points $E$ and $W$, at which $g$ has already been determined. Similarly, the value of $(V/r)_{,r}$ at the center of $\Sigma$ can be approximated to second order in terms of values of $V$ at points where it can be determined by integrating the hypersurface equations (5) and (6) radially outward from $r = 0$.

After carrying out this procedure to evaluate $g$ at the point $N$, the procedure

can then be iterated to determine $g$ at the next radially outward grid point on the $u_0 + \Delta u$ level, i.e. point $n$ in Fig. 2. Upon completing this radial march to null infinity, in terms of a compactified radial coordinate such as $x = r/(1+r)$, the field $g$ is then evaluated on the next null cone at $u_0 + 2\Delta u$, beginning at the vertex where smoothness gives the startup condition that $g(u, 0) = 0$.

In the compactified Bondi formalism, the vertices $N$, $E$, $S$ and $W$ of the null parallelogram $\Sigma$ cannot be chosen to lie exactly on the grid because, even in Minkowski space, the velocity of light in terms of a compactified radial coordinate $x$ is not constant. As a consequence, the fields $g$, $\beta$ and $V$ at the vertices of $\Sigma$ are approximated to second order accuracy by interpolating between grid points. However, cancellations arise between these four interpolations so that Eq. (8) is satisfied to fourth order accuracy. The net result is that the finite difference version of (8) steps $g$ radially outward one zone with an error of fourth order in grid size, $O((\Delta u)^2(\Delta x)^2)$. In addition, the smoothness conditions (4) can be incorporated into the startup for the numerical integrations for $V$ and $\beta$ to insure no loss of accuracy in starting up the march at $r = 0$. The resulting global error in $g$, after evolving a finite retarded time, is then $O(\Delta u \Delta x)$, after compounding errors from $1/(\Delta u \Delta x)$ number of zones.

When implemented on a grid based upon the $(u, r)$ coordinates, the stability of this algorithm is subject to a Courant-Friedrichs-Lewy (CFL) condition requiring that the physical domain of dependence be contained in the numerical domain of dependence. In the spherically symmetric case, this condition requires that the ratio of the time step to radial step be limited by $(V/r)\Delta u \leq 2\Delta r$, where $\Delta r = \Delta[x/(1-x)]$. This condition can be built into the code using the value $V/r = e^{2H}$, corresponding to the maximum of $V/r$ at $\mathcal{I}^+$. The strongest restriction on the time step then arises just before the formation of a horizon, where $V/r \to \infty$ at $\mathcal{I}^+$. This infinite redshift provides a mechanism for locating the true event horizon "on the fly" and restricting the evolution to the exterior spacetime. Points near $\mathcal{I}^+$ must be dropped in order to evolve across the horizon due to the lack of a nonsingular compactified version of future time infinity $I^+$.

The situation is quite different in a double null coordinate system, in which the vertices of the null parallelogram can be placed exactly on grid points so that the CFL condition is automatically satisfied. A characteristic code based upon double null coordinates was used by Goldwirth and Piran in a study of cosmic censorship [67] based upon the spherically symmetric gravitational collapse of a scalar field. Their early study lacked the sensitivity of adaptive mesh refinement which later enabled Choptuik to discover the critical phenomena appearing in this problem. Subsequent work by Marsa and Choptuik [103] combined the use of the null related ingoing Eddington-Finklestein coordinates with singularity excision to construct a 1D code that "runs forever". Later, Garfinkle [63] constructed an improved version of the Goldwirth-Piran double null code which was able to simulate critical phenomena without using adaptive mesh refinement. In this treatment, as the evolution proceeds on one outgoing null cone to the next, the grid points follow the ingoing null cones and must be dropped as they cross the origin at $r = 0$. However, after half the grid points are lost they are then

"recycled" at new positions midway the remaining grid points. This technique is crucial to resolving the critical phenomena associated with an $r \to 0$ sized horizon. An extension of the code [64] was later used to verify that scalar field collapse in six dimensions continues to display critical phenomena.

Hamadé and Stewart [84] also applied a double null code to study critical phenomena. In order to obtain the accuracy necessary to confirm Choptuik's results they developed the first example of a characteristic grid with adaptive mesh refinement (AMR). They did this with both the standard Berger and Oliger algorithm and their own simplified version, with both versions giving indistinguishable results. Their simulations of critical collapse of a scalar field agreed with Choptuik's values for the universal parameters governing mass scaling and displayed the echoing associated with discrete self-similarity. Hamadé, Horne and Stewart [83] extended this study to the spherical collapse of an axion/dilaton system and found in this case that the self-similarity was a continuous symmetry of the critical solution.

A code based upon Bondi coordinates, developed by S. Husa and his collaborators [88], has been successfully applied to spherically symmetric critical collapse of a nonlinear $\sigma$-model coupled to gravity. Critical phenomena cannot be resolved on a static grid based upon the Bondi $r$-coordinate. Instead, the numerical techniques of Garfinkle were adopted by using a dynamic grid following the ingoing null rays and by recycling radial grid points. They studied how coupling to gravity affects the critical behavior previously observed by P. Bizoń [32] and others in the Minkowski space version of the model. For a wide range of the coupling constant, they observe discrete self-similarity and typical mass scaling near the critical solution. The code is shown to be second order accurate and to give second order convergence for the value of the critical parameter.

The first characteristic code in Bondi coordinates for the self-gravitating scalar wave problem was constructed by Gómez and Winicour [76]. They introduced a numerical compactification of $\mathcal{I}^+$ for the purpose of studying effects of self-gravity on the scalar radiation, particularly in the high amplitude limit of the rescaling $\Phi \to a\Phi$. As $a \to \infty$, the red shift creates an effective boundary layer at $\mathcal{I}^+$ which causes the Bondi mass $M_{\rm B}$ and the scalar field monopole moment $Q$ to be related by $M_{\rm B} \sim \pi|Q|/\sqrt{2}$, rather than the quadratic relation of the weak field limit [76]. This could also be established analytically so that the high amplitude limit provided a check on the code's ability to handle strongly nonlinear fields. In the small amplitude case, this work *incorrectly* reported that the radiation tails from black hole formation had an exponential decay characteristic of quasinormal modes rather than the polynomial $1/t$ or $1/t^2$ falloff expected from Price's [116] work on perturbations of Schwarzschild black holes. In hindsight, the error here was not having confidence to run the code sufficiently long to see the proper late time behavior.

Gundlach, Price and Pullin [80, 81] subsequently reexamined the issue of power law tails using a double null code similar to that developed by Goldwirth and Piran. Their numerical simulations verified the existence of power law tails in the full nonlinear case, thus establishing consistency with analytic perturbative theory. They also found normal mode ringing at intermediate time, which

provided reassuring consistency with perturbation theory and showed that there is a region of spacetime where the results of linearized theory are remarkably reliable even though highly nonlinear behavior is taking place elsewhere. These results have led to a methodology that has application beyond the confines of spherically symmetric problems, most notably in the "close approximation" for the binary black hole problem [117]. Power law tails and quasinormal ringing were also confirmed using Cauchy evolution [103].

The study of the radiation tail decay of a scalar field was subsequently extended by Gómez, Schmidt and Winicour [75] using a characteristic code. They showed that the Newman-Penrose constant [108] for the scalar field determines the exponent of the power law (not the static monopole moment as often stated). When this constant is non-zero, the tail decays as $1/t$, as opposed to the $1/t^2$ decay for the vanishing case. (There are also $t^{-n}\log t$ corrections in addition to the exponentially decaying contributions of the quasinormal modes.) This code was also used to study the instability of a topological kink in the configuration of the scalar field [13]. The kink instability provides the simplest example of the turning point instability [90, 129] which underlies gravitational collapse of static equilibria.

The Southampton group has constructed a $\{1+1\}$-dimensional characteristic code for spacetimes with cylindrical symmetry [46, 54]. The original motivation was to use it as the exterior characteristic code in a test case of Cauchy-characteristic matching (CCM). (See Sec. 4.4.1 of this review for the application to matching.) However, U. Sperhake, K. R. P. Sjödin and J. A. Vickers [130, 131] have recently modified the code into a global characteristic version for the purpose of studying cosmic strings, represented by massive scalar and vector fields coupled to gravity. Using a Geroch decomposition [65] with respect to the translational Killing vector, the global problem is reduced to a $\{2+1\}$-dimensional asymptotically flat spacetime, so that $\mathcal{I}^+$ can be compactified and included in the numerical grid. Rather than the explicit scheme used in CCM, the new version employs an implicit, second order in space and time, Crank-Nicholson evolution scheme. The code showed long term stability and second order convergence in vacuum tests based upon exact Weber-Wheeler waves [152], Xanthopoulos' rotating solution [155], and in tests of wave scattering by a string. The results show damped ringing of the string after a incoming Weber-Wheeler pulse has excited it and scattered out to $\mathcal{I}^+$. The ringing frequencies are independent of the details of the pulse but are inversely proportional to the masses of the scalar and vector fields.

The group at the Universidad de Oriente in Venezuela has applied characteristic methods to study the self-similar collapse of spherical matter and charge distributions [11, 14, 12]. The assumption of self-similarity reduces the problem to a system of ODE's, subject to boundary conditions determined by matching to an exterior Reissner-Nordstrom-Vaidya solution. Heat flow in the internal fluid is balanced at the surface by the Vaidya radiation. Their solutions illustrate how a nonzero total charge can halt gravitational collapse and produce a final stable equilibrium [12]. It is interesting that the pressure vanishes in the final equilibrium state so that hydrostatic support is completely supplied by

Coulomb repulsion.

## 3.2 {2 + 1} Codes

One-dimensional characteristic codes enjoy a very special simplicity due to the two preferred sets (ingoing and outgoing) of characteristic null hypersurfaces. This eliminates a source of gauge freedom that otherwise exists in either two- or three-dimensional characteristic codes. However, the manner in which characteristics of a hyperbolic system determine domains of dependence and lead to propagation equations for shock waves is the same as in the one-dimensional case. This makes it desirable for the purpose of numerical evolution to enforce propagation along characteristics as extensively as possible. In basing a Cauchy algorithm upon shooting along characteristics, the infinity of characteristic rays (technically, *bicharacteristics*) at each point leads to an arbitrariness which, for a practical numerical scheme, makes it necessary either to average the propagation equations over the sphere of characteristic directions or to select out some preferred subset of propagation equations. The latter approach was successfully applied by Butler [37] to the Cauchy evolution of two-dimensional fluid flow but there seems to have been very little follow-up along these lines.

The formal ideas behind the construction of two- or three-dimensional characteristic codes are the same, although there are different technical choices of angular coordinates for the null rays. Historically, most characteristic work graduated first from 1D to 2D because of the available computing power.

## 3.3 The Bondi Problem

The first characteristic code based upon the original Bondi equations for a twist-free axisymmetric spacetime was constructed by Isaacson, Welling and Winicour [92] at Pittsburgh. The spacetime was foliated by a family of null cones, complete with point vertices at which regularity conditions were imposed. The code accurately integrated the hypersurface and evolution equations out to compactified null infinity. This allowed studies of the Bondi mass and radiation flux on the initial null cone, but it could not be used as a practical evolution code because of an instability at the vertices of the null cones.

These instabilities came as a rude shock and led to a retreat to the simpler problem of axisymmetric scalar waves propagating in Minkowski space, with the metric

$$ds^2 = -du^2 - 2dudr + r^2(d\theta^2 + \sin^2\theta d\phi^2) \tag{9}$$

in outgoing null cone coordinates. A null cone code for this problem was constructed using an algorithm based upon Eq. (8), with the angular part of the flat space Laplacian replacing the curvature terms in the integrand on the right hand side. This simple setting allowed the instability to be traced to a subtle violation of the CFL condition near the vertices of the cones. In terms of grid spacings $\Delta x^\alpha$, the CFL condition in this coordinate system takes the explicit form

$$\Delta u/\Delta r < -1 + [K^2 + (K-1)^2 - 2K(K-1)\cos\Delta\theta]^{1/2}, \tag{10}$$

where the coefficient $K$, which is of order 1, depends on the particular startup procedure adopted for the outward integration. Far from the vertex, the condition (10) on the time step $\Delta u$ is quantitatively similar to the CFL condition for a standard Cauchy evolution algorithm in spherical coordinates. But condition (10) is strongest near the vertex of the cone where (at the equator $\theta = \pi/2$) it implies that

$$\Delta u < K \Delta r (\Delta\theta)^2. \tag{11}$$

This is in contrast to the analogous requirement

$$\Delta u < K \Delta r \Delta\theta \tag{12}$$

for stable Cauchy evolution near the origin of a spherical coordinate system. The extra power of $\Delta\theta$ is the price that must be paid near the vertex for the simplicity of a characteristic code. Nevertheless, the enforcement of this condition allowed efficient global simulation of axisymmetric scalar waves. Global studies of backscattering, radiative tail decay and solitons were carried out for nonlinear axisymmetric waves [92], but three-dimensional simulations extending to the vertices of the cones were impractical on existing machines.

Aware now of the subtleties of the CFL condition near the vertices, the Pittsburgh group returned to the Bondi problem, i.e. to evolve the Bondi metric [35]

$$\begin{aligned} ds^2 = &\left(\frac{V}{r} e^{2\beta} - U^2 r^2 e^{2\gamma}\right) du^2 + 2 e^{2\beta} du dr + \ 2U r^2 e^{2\gamma} du d\theta \\ &- r^2 (e^{2\gamma} d\theta^2 + e^{-2\gamma} \sin^2\theta d\phi^2), \end{aligned} \tag{13}$$

by means of the three hypersurface equations

$$\beta_{,r} = \frac{1}{2} r \, (\gamma_{,r})^2, \tag{14}$$

$$[r^4 \, e^{2(\gamma-\beta)} U_{,r}]_{,r} = 2 r^2 \left[ r^2 \left(\frac{\beta}{r^2}\right)_{,r\theta} - \frac{(\sin^2\theta \, \gamma)_{,r\theta}}{\sin^2\theta} + 2 \, \gamma_{,r} \, \gamma_{,\theta} \right], \tag{15}$$

$$\begin{aligned} V_{,r} = &-\frac{1}{4} r^4 e^{2(\gamma-\beta)} (U_{,r})^2 + \frac{(r^4 \sin\theta U)_{,r\theta}}{2 r^2 \sin\theta} \\ &+ e^{2(\beta-\gamma)} \Bigg[ 1 - \frac{(\sin\theta \beta_{,\theta})_{,\theta}}{\sin\theta} + \gamma_{,\theta\theta} + 3 \cot\theta \gamma_{,\theta} - (\beta_{,\theta})^2 \\ &- 2 \gamma_{,\theta} (\gamma_{,\theta} - \beta_{,\theta}) \Bigg], \end{aligned} \tag{16}$$

and the evolution equation

$$\begin{aligned} 4 r (r\gamma)_{,ur} = &\left[ 2 r \gamma_{,r} V - r^2 \left( 2 \gamma_{,\theta} \, U + \sin\theta \left( \frac{U}{\sin\theta} \right)_{,\theta} \right) \right]_{,r} - 2 r^2 \frac{(\gamma_{,r} U \sin\theta)_{,\theta}}{\sin\theta} \\ &+ \frac{1}{2} r^4 e^{2(\gamma-\beta)} (U_{,r})^2 + 2 e^{2(\beta-\gamma)} \left[ (\beta_{,\theta})^2 + \sin\theta \left( \frac{\beta_{,\theta}}{\sin\theta} \right)_{,\theta} \right]. \end{aligned} \tag{17}$$

The beauty of the Bondi equations is that they form a clean hierarchy. Given $\gamma$ on an initial null hypersurface, the equations can be integrated radially to determine $\beta$, $U$, $V$ and $\gamma_{,u}$ on the hypersurface (in that order) in terms of integration constants determined by boundary conditions, or smoothness if extended to the vertex of a null cone. The initial data $\gamma$ is unconstrained except by smoothness conditions. Because $\gamma$ represents a spin-2 field, it must be $O(\sin^2\theta)$ near the poles of the spherical coordinates and must consist of $l \geq 2$ spin-2 multipoles.

In the computational implementation of this system by the Pittsburgh group [74], the null hypersurfaces were chosen to be complete null cones with nonsingular vertices, which (for simplicity) trace out a geodesic worldline $r = 0$. The smoothness conditions at the vertices were formulated in local Minkowski coordinates.

The vertices of the cones were not the chief source of difficulty. A null parallelogram marching algorithm, similar to that used in the scalar case, gave rise to an instability that sprang up throughout the grid. In order to reveal the source of the instability, physical considerations suggested looking at the linearized version of the Bondi equations, since they must be related to the wave equation. If this relationship were sufficiently simple, then the scalar wave algorithm could be used as a guide in stabilizing the evolution of $\gamma$. A scheme for relating $\gamma$ to solutions $\Phi$ of the wave equation had been formulated in the original paper by Bondi, Metzner and van den Burgh [35]. However, in that scheme, the relationship of the scalar wave to $\gamma$ was nonlocal in the angular directions and was not useful for the stability analysis.

A local relationship between $\gamma$ and solutions of the wave equation was found [74]. This provided a test bed for the null evolution algorithm similar to the Cauchy test bed provided by Teukolsky waves [140]. More critically, it allowed a simple von Neumann linear stability analysis of the finite difference equations, which revealed that the evolution would be unstable if the metric quantity $U$ was evaluated on the grid. For a stable algorithm, the grid points for $U$ must be staggered between the grid points for $\gamma$, $\beta$ and $V$. This unexpected feature emphasizes the value of linear stability analysis in formulating stable finite difference approximations.

It led to an axisymmetric code for the global Bondi problem which ran stably, subject to a CFL condition, throughout the regime in which caustics and horizons did not form. Stability in this regime was verified experimentally by running arbitrary initial data until it radiated away to $\mathcal{I}^+$. Also, new exact solutions as well as the linearized null solutions were used to perform extensive convergence tests that established second order accuracy. The code generated a large complement of highly accurate numerical solutions for the class of asymptotically flat, axisymmetric vacuum spacetimes, a class for which no analytic solutions are known. All results of numerical evolutions in this regime were consistent with the theorem of Christodoulou and Klainerman [44] that weak initial data evolve asymptotically to Minkowski space at late time.

An additional global check on accuracy was performed using Bondi's formula

relating mass loss to the time integral of the square of the news function. The Bondi mass loss formula is not one of the equations used in the evolution algorithm but follows from those equations as a consequence of a global integration of the Bianchi identities. Thus it not only furnishes a valuable tool for physical interpretation but it also provides a very important calibration of numerical accuracy and consistency.

An interesting feature of the evolution arises in regard to compactification. By construction, the $u$-direction is timelike at the origin where it coincides with the worldline traced out by the vertices of the outgoing null cones. But even for weak fields, the $u$-direction generically becomes spacelike at large distances along an outgoing ray. Geometrically, this reflects the property that $\mathcal{I}$ is itself a null hypersurface so that all internal directions are spacelike, except for the null generator. For a flat space time, the $u$-direction picked out at the origin leads to a null evolution direction at $\mathcal{I}$, but this direction becomes spacelike under a slight deviation from spherical symmetry. Thus the evolution generically becomes "superluminal" near $\mathcal{I}$. Remarkably, there were no adverse numerical effects. This fortuitous property apparently arises from the natural way that causality is built into the marching algorithm so that no additional resort to numerical techniques, such as "causal differencing" [141], was necessary.

### 3.3.1 The Conformal-Null Tetrad Approach

J. Stewart has implemented a characteristic evolution code which handles the Bondi problem by a null tetrad, as opposed to metric, formalism [135]. The geometrical algorithm underlying the evolution scheme, as outlined in [136, 62], is H. Friedrich's [59] conformal-null description of a compactified spacetime in terms of a first order system of partial differential equations. The variables include the metric, the connection, and the curvature, as in a Newman-Penrose formalism, but in addition the conformal factor (necessary for compactification of $\mathcal{I}$) and its gradient. Without assuming any symmetry, there are more than 7 times as many variables as in a metric based null scheme, and the corresponding equations do not decompose into as clean a hierarchy. This disadvantage, compared to the metric approach, is balanced by several advantages:

1. The equations form a symmetric hyperbolic system so that standard theorems can be used to establish that the system is well-posed.

2. Standard evolution algorithms can be invoked to ensure numerical stability.

3. The extra variables associated with the curvature tensor are not completely excess baggage, since they supply essential physical information.

4. The regularization necessary to treat $\mathcal{I}$ is built in as part of the formalism so that no special numerical regularization techniques are necessary as in the metric case. (This last advantage is somewhat offset by the necessity of having to locate $\mathcal{I}$ by tracking the zeroes of the conformal factor.)

The code was intended to study gravitational waves from an axisymmetric star. Since only the vacuum equations are evolved, the outgoing radiation from the star is represented by data ($\Psi_4$ in Newman-Penrose notation) on an ingoing null cone forming the inner boundary of the evolved domain. The inner boundary data is supplemented by Schwarzschild data on the initial outgoing null cone, which models an initially quiescent state of the star. This provides the necessary data for a double-null initial value problem. The evolution would normally break down where the ingoing null hypersurface develops caustics. But by choosing a scenario in which a black hole is formed, it is possible to evolve the entire region exterior to the horizon. An obvious test bed is the Schwarzschild spacetime for which a numerically satisfactory evolution was achieved (convergence tests were not reported).

Physically interesting results were obtained by choosing data corresponding to an outgoing quadrupole pulse of radiation. By increasing the initial amplitude of the data $\Psi_4$, it was possible to evolve into a regime where the energy loss due to radiation was large enough to drive the total Bondi mass negative. Although such data is too grossly exaggerated to be consistent with an astrophysically realistic source, the formation of a negative mass is an impressive test of the robustness of the code.

### 3.3.2 Twisting Axisymmetry

The Southampton group, as part of its long range goal of combining Cauchy and characteristic evolution has developed a code [52, 53, 115] which extends the Bondi problem to full axisymmetry, as described by the general characteristic formalism of Sachs [122]. By dropping the requirement that the rotational Killing vector be twist-free, they are able to include rotational effects, including radiation in the "cross" polarization mode (only the "plus" mode is allowed by twist-free axisymmetry). The null equations and variables are recast into a suitably regularized form to allow compactification of null infinity. Regularization at the vertices or caustics of the null hypersurfaces is not necessary, since they anticipate matching to an interior Cauchy evolution across a finite worldtube.

The code is designed to insure Bondi coordinate conditions at infinity, so that the metric has the asymptotically Minkowskian form corresponding to null-spherical coordinates. In order to achieve this, the hypersurface equation for the Bondi metric variable $\beta$ must be integrated radially inward from infinity, where the integration constant is specified. The evolution of the dynamical variables proceeds radially outward as dictated by causality [115]. This differs from the Pittsburgh code in which all the equations are integrated radially outward, so that the coordinate conditions are determined at the inner boundary and the metric is asymptotically flat but not asymptotically Minkowskian. The Southampton scheme simplifies the formulae for the Bondi news function and mass in terms of the metric. It is anticipated that the inward integration of $\beta$ causes no numerical problems because this is a gauge choice which does not propagate physical information. However, the code has not yet been subject to convergence and long term stability tests so that these issues cannot be properly

assessed at the present time.

The matching of the Southampton axisymmetric code to a Cauchy interior is discussed in Sec. 4.5.

## 3.4 The Bondi Mass

Numerical calculations of asymptotic quantities such as the Bondi mass must overcome severe technical difficulties arising from the necessity to pick off non-leading terms in an asymptotic expansion about infinity. For example, in an asymptotically inertial frame (called a Bondi frame at $\mathcal{I}^+$), the mass aspect $\mathcal{M}(u,\theta,\phi)$ must be picked off from the asymptotic expansion of Bondi's metric quantity $V$ (see Eq. (16)) of the form $V = r - 2\mathcal{M} + O(1/r)$. This is similar to the experimental task of determining the mass of an object by measuring its far field. The job is more difficult if the gauge choice does not correspond to a Bondi frame at $\mathcal{I}^+$. One must then deal with an arbitrary foliation of $\mathcal{I}^+$ into retarded time slices which are determined by the details of the interior geometry. As a result, $V$ has the more complicated asymptotic behavior, given in the axisymmetric case by

$$\begin{aligned} V - r = {} & r^2 (L \sin\theta)_{,\theta} / \sin\theta + r e^{2(H-K)} \Big[ (1 - e^{-2(H-K)}) \\ & + 2(H_{,\theta} \sin\theta)_{,\theta} / \sin\theta + K_{,\theta\theta} + 3K_{,\theta} \cot\theta + 4(H_{,\theta})^2 \\ & - 4H_{,\theta} K_{,\theta} - 2(K_{,\theta})^2 \Big] - 2e^{2H} \mathcal{M} + O(r^{-1}), \end{aligned} \tag{18}$$

where $L$, $H$ and $K$ are gauge dependent functions of $(u,\theta)$ which would vanish in a Bondi frame [139, 92]. The calculation of the Bondi mass requires regularization of this expression by numerical techniques so that the coefficient $\mathcal{M}$ can be picked off. The task is now similar to the experimental determination of the mass of an object by using non-inertial instruments in a far zone which contains $O(1/r)$ radiation fields. But it can be done!

It was accomplished in Stewart's code by reexpressing the formula for the Bondi mass in terms of the well-behaved fields of the conformal formalism [135]. In the Pittsburgh code, it was accomplished by re-expressing the Bondi mass in terms of renormalized metric variables which regularize all calculations at $\mathcal{I}^+$ and make them second order accurate in grid size [69]. The calculation of the Bondi news function (which provides the waveforms of both polarization modes) is an easier numerical task than the Bondi mass. It has also been implemented in both of these codes, thus allowing the important check of the Bondi mass loss formula.

An alternative approach to computing the Bondi mass is to adopt a gauge which corresponds more closely to an inertial or Bondi frame at $\mathcal{I}^+$ and simplifies the asymptotic limit. Such a choice is the null quasi-spherical gauge in which the angular part of the metric is proportional to the unit sphere metric and as a result the gauge term $K$ vanishes in Eq. (18). This gauge was adopted by the Canberra group in developing a 3-D characteristic evolution code [21] (see

Sec. 3.5 for further discussion). It allowed accurate computation of the Bondi mass as a limit as $r \to \infty$ of the Hawking mass [17].

Mainstream astrophysics is couched in Newtonian concepts, some of which have no well defined extension to general relativity. In order to provide a sound basis for relativistic astrophysics, it is crucial to develop general relativistic concepts which have well defined and useful Newtonian limits. Mass and radiation flux are fundamental in this regard. The results of characteristic codes show that the energy of a radiating system can be evaluated rigorously and accurately according to the rules for asymptotically flat spacetimes, while avoiding the deficiencies that plagued the "pre-numerical" era of relativity: (i) the use of coordinate dependent concepts such as gravitational energy-momentum pseudotensors; (ii) a rather loose notion of asymptotic flatness, particularly for radiative spacetimes; (iii) the appearance of divergent integrals; and (iv) the use of approximation formalisms, such as weak field or slow motion expansions, whose errors have not been rigorously estimated.

Characteristic codes have extended the role of the Bondi mass from that of a geometrical construct in the theory of isolated systems to that of a highly accurate computational tool. The Bondi mass loss formula provides an important global check on the preservation of the Bianchi identities. The mass loss rates themselves have important astrophysical significance. The numerical results demonstrate that computational approaches, rigorously based upon the geometrical definition of mass in general relativity, can be used to calculate radiation losses in highly nonlinear processes where perturbation calculations would not be meaningful.

Numerical calculation of the Bondi mass has been used to explore both the Newtonian and the strong field limits of general relativity [69]. For a quasi-Newtonian system of radiating dust, the numerical calculation joins smoothly on to a post-Newtonian expansion of the energy in powers of $1/c$, beginning with the Newtonian mass and mechanical energy as the leading terms. This comparison with perturbation theory has been carried out to $O(1/c^7)$, at which stage the computed Bondi mass peels away from the post-Newtonian expansion. It remains strictly positive, in contrast to the truncated post-Newtonian behavior which leads to negative values.

A subtle feature of the Bondi mass stems from its role as one component of the total energy-momentum 4-vector, whose calculation requires identification of the translation subgroup of the Bondi-Metzner-Sachs group [121]. This introduces boost freedom into the problem. Identifying the translation subgroup is tantamount to knowing the conformal transformation to a conformal Bondi frame [139] in which the time slices of $\mathcal{I}$ have unit sphere geometry. Both Stewart's code and the Pittsburgh code adapt the coordinates to simplify the description of the interior sources. This results in an arbitrary foliation of $\mathcal{I}$. The determination of the conformal factor which relates the 2-metric $h_{AB}$ of a slice of $\mathcal{I}$ to the unit sphere metric is an elliptic problem equivalent to solving the second order partial differential equation for the conformal transformation of Gaussian curvature. In the axisymmetric case, the PDE reduces to an ODE with respect to the angle $\theta$, and is straightforward to solve [69]. The integration

constants determine the boost freedom along the axis of symmetry.

The non-axisymmetric case is more complicated. Stewart [135] proposes an approach based upon the dyad decomposition

$$h_{AB}dx^A dx^B = m_A dx^A \bar{m}_B dx^B. \tag{19}$$

The desired conformal transformation is obtained by first relating $h_{AB}$ conformally to the flat metric of the complex plane. Denoting the complex coordinate of the plane by $\zeta$, this relationship can be expressed as $d\zeta = e^f m_A dx^A$. The conformal factor $f$ can then be determined from the integrability condition

$$m_{[A}\partial_{B]}f = \partial_{[A}m_{B]}. \tag{20}$$

This is equivalent to the classic Beltrami equation for finding isothermal coordinates. It would appear to be a more effective scheme than tackling the second order PDE directly, but numerical implementation has not yet been carried out.

## 3.5 3D Characteristic Evolution

There has been rapid progress in 3D characteristic evolution. There are now two independent 3D codes, one developed at Canberra and the other at Pittsburgh (the PITT code), which have the capability to study gravitational waves in single black hole spacetimes, at a level still not mastered by Cauchy codes. Three years ago the Pittsburgh group established robust stability and second order accuracy of a fully nonlinear 3D code which calculates waveforms at null infinity [31, 30] and also tracks a dynamical black hole and excises its internal singularity from the computational grid [73, 70]. The Canberra group has implemented an independent nonlinear 3D code which accurately evolves the exterior region of a Schwarzschild black hole. Both codes pose data on an initial null hypersurface and on a worldtube boundary, and evolve the exterior spacetime out to a compactified version of null infinity, where the waveform is computed. However, there are essential differences in the underlying geometrical formalisms and numerical techniques used in the two codes and their success in evolving generic black hole spacetimes.

### 3.5.1 Geometrical formalism

The PITT code uses a standard Bondi-Sachs null coordinate system whereas the Canberra code employs a null quasi-spherical (NQS) gauge (not to be confused with the quasi-spherical approximation in which quadratically aspherical terms are ignored [31]). The NQS gauge takes advantage of the possibility of mapping the angular part of the Bondi metric conformally onto a unit sphere metric, so that $h_{AB} \to q_{AB}$. The required transformation $x^A \to y^A(u, r, x^A)$ is in general dependent upon $u$ and $r$ so that the quasi-spherical angular coordinates $y^A$ are not constant along the outgoing null rays, unlike the Bondi-Sachs angular coordinates. Instead the coordinates $y^A$ display the analogue of a shift on the null hypersurfaces $u = \text{const.}$. The radiation content of the metric is contained

in a shear vector describing this shift. This results in the description of the radiation in terms of a spin-weight 1 field, rather than the spin-weight 2 field associated with $h_{AB}$ in the Bondi-Sachs formalism. In both the Bondi-Sachs and NQS gauges, the independent gravitational data on a null hypersurface is the conformal part of its degenerate 3-metric. The Bondi-Sachs null data consists of $h_{AB}$, which determines the intrinsic conformal metric of the null hypersurface. In the quasi-spherical case, $h_{AB} = q_{AB}$ and the shear vector comprises the only non-trivial part of the conformal 3-metric. Both the Bondi-Sachs and NQS gauges can be arranged to coincide in the special case of shear-free Robinson-Trautman metrics [49, 16].

The formulation of Einstein's equations in the NQS gauge is presented in Ref. [15] and the associated gauge freedom arising from $(u, r)$ dependent rotation and boosts of the unit sphere is discussed in Ref. [16]. As in the PITT code, the main equations involve integrating a hierarchy of hypersurface equations along the radial null geodesics extending from the inner boundary to null infinity. In the NQS gauge the source terms for these radial ODE's are rather simple when the unknowns are chosen to be the connection coefficients. However, as a price to pay for this simplicity, after the radial integrations are performed on each null hypersurface a first order elliptic equation must be solved on each $r =$ const. cross-section to reconstruct the underlying metric.

### 3.5.2 Numerical Methodology

The PITT code is an explicit second order finite difference evolution algorithm based upon retarded time steps on a uniform three-dimensional null coordinate grid. The straightforward numerical approach and the second order convergence of the finite difference equations has facilitated code development. The Canberra code uses an assortment of novel and elegant numerical methods. Most of these involve smoothing or filtering and have obvious advantage for removing short wavelength noise but would be unsuitable for modeling shocks.

Both codes require the ability to handle tensor fields and their derivatives on the sphere. Spherical coordinates and spherical harmonics are natural analytic tools for the description of radiation but their implementation in computational work requires dealing with the impossibility of smoothly covering the sphere with a single coordinate grid. Polar coordinate singularities in axisymmetric systems can be regularized by standard tricks. In the absence of symmetry, these techniques do not generalize and would be especially prohibitive to develop for tensor fields.

A crucial ingredient of the PITT code is the *eth*-module [72] which incorporates a computational version of the Newman-Penrose eth-formalism [107]. The eth-module covers the sphere with two overlapping stereographic coordinate grids (North and South). It provides everywhere regular, second order accurate, finite difference expressions for tensor fields on the sphere and their covariant derivatives. The eth-calculus simplifies the underlying equations, avoids spurious coordinate singularities and allows accurate differentiation of tensor fields on the sphere in a computationally efficient and clean way. Its main weakness

is the numerical noise introduced by interpolations (4th order accurate) between the North and South patches. For parabolic or elliptic equations on the sphere, the finite difference approach of the eth-calculus would be less efficient than a spectral approach, but no parabolic or elliptic equations appear in the Bondi-Sachs evolution scheme.

The Canberra code handles fields on the sphere by means of a 3-fold representation [20]: (i) discretized functions on a spherical grid uniformly spaced in standard $(\theta, \phi)$ coordinates, (ii) fast-Fourier transforms with respect to $(\theta, \phi)$ (based upon a smooth map of the torus onto the sphere), and (iii) spectral decomposition of scalar, vector and tensor fields in terms of spin-weighted spherical harmonics. The grid values are used in carrying out nonlinear algebraic operations; the Fourier representation is used to calculate $(\theta, \phi)$-derivatives; and the spherical harmonic representation is used to solve global problems, such as the solution of the first order elliptic equation for the reconstruction of the metric, whose unique solution requires pinning down the $\ell = 1$ gauge freedom. The sizes of the grid and of the Fourier and spherical harmonic representations are coordinated. In practice, the spherical harmonic expansion is carried out to 15th order in $\ell$ but the resulting coefficients must then be projected into the $\ell \leq 10$ subspace in order to avoid inconsistencies between the spherical harmonic and the grid and Fourier representations.

The Canberra code solves the null hypersurface equations by combining an 8th order Runge-Kutta integration with a convolution spline to interpolate field values. The radial grid points are dynamically positioned to approximate ingoing null geodesics, a technique originally due to Goldwirth and Piran [67] to avoid inaccuracies near a horizon resulting from a uniform $r$-grid due to the coordinate singularity in the case of a stationary horizon. The time evolution uses the method of lines with a 4th order Runge-Kutta integrator, which introduces further high frequency filtering.

### 3.5.3 Stability

**PITT Code**: Analytic stability analysis of the finite difference equations has been crucial in the development of a stable evolution algorithm, subject to the standard Courant-Friedrichs-Lewy (CFL) condition for an explicit code. Linear stability analysis on Minkowski and Schwarzschild backgrounds showed that certain field variables must be represented on the half-grid [74, 31]. Nonlinear stability analysis was essential in revealing and curing a mode coupling instability that was not present in the original axisymmetric version of the code [30, 98]. Stability persists even in the regime that the $u$-direction, along which the grid flows, becomes spacelike, such as outside the velocity of light cone in a rotating coordinate system. Severe tests were used to verify stability. In the linear regime, **robust stability** was established by imposing random initial data on the initial characteristic hypersurface and random constraint violating boundary data on an inner worldtube. The code ran stably for 10,000 grid crossing times under these conditions [31, 138]. Except for a linearized version of an Arnowitt-Deser-Misner code [138] (see also Sec. 4), the PITT code is the only

3D general relativistic code which has passed this test of robust stability. The use of random data is only possible in sufficiently weak cases where effective energy terms quadratic in the field gradients are not dominant. Stability in the highly nonlinear regime was tested in two ways. Runs for a time of 60,000 $M$ were carried out for a moving, distorted Schwarzschild black hole (of mass $M$), with the marginally trapped surface at the inner boundary tracked and its interior excised from the computational grid [70, 143]. This is the longest black hole simulation carried out to date. Furthermore, the scattering of a gravitational wave off a Schwarzschild black hole was successfully carried out in the extreme nonlinear regime where the backscattered Bondi news was as large as $N = 400$ (in dimensionless geometric units) [30], showing that the code can cope with the enormous power output $N^2c^5/G \approx 10^{60}$ W in conventional units. This exceeds the power that would be produced if, in 1 second, the entire galaxy were converted to gravitational radiation.

**Canberra code**: Direct stability analysis of the underlying finite difference equations is impractical because of the extensive mix of spectral techniques, higher order methods and splines. Similarly, there is no clear-cut CFL limit on the code, although stability tests show that there is a limit on the time step. The damping of high frequency modes due to the implicit filtering would be expected to suppress numerical instability, but the stability of the Canberra code is nevertheless subject to two qualifications [18, 19, 21]: (i) At late times (less than 100 $M$), the evolution terminates as it approaches an event horizon, apparently because of a breakdown of the NQS gauge condition, although an analysis of how and why this should occur has not yet been given. (ii) Numerical instabilities arise from dynamic inner boundary conditions and restrict the inner boundary to a fixed Schwarzschild horizon. Tests in the extreme nonlinear regime were not reported.

### 3.5.4 Accuracy

**PITT Code**: Second order accuracy was verified in an extensive number of testbeds [31, 30, 70], including new exact solutions specifically constructed in null coordinates for the purpose of convergence tests:

- Linearized waves on a Minkowski background in null cone coordinates.
- Boost and rotation symmetric solutions [23].
- Schwarzschild in rotating coordinates.
- Polarization symmetry of nonlinear twist-free axisymmetric waveforms.
- Robinson-Trautman waveforms from perturbed Schwarzschild black holes.
- Nonlinear Robinson-Trautman waveforms utilizing an independently computed solution of the Robinson-Trautman equation.

**Canberra code**: The complexity of the algorithm and NQS gauge makes it problematic to establish accuracy by direct means. Exact solutions do not provide an effective convergence check because the Schwarzschild solution is trivial in the NQS gauge and other known solutions in this gauge require dynamic inner boundary conditions which destabilize the present version of the code. Convergence to linearized solutions is a possible check but has not yet been performed. Instead indirect tests by means of geometric consistency and partial convergence tests are used to calibrate accuracy. The consistency tests are based on the constraint equations, which are not enforced during null evolution except at the inner boundary. The balance between mass loss and radiation flux through $\mathcal{I}^+$ is a global version of these constraints. No appreciable growth of the constraints is noticeable until within 5 $M$ of the final breakdown of the code. In weak field tests where angular resolution does not dominate the error, partial convergence tests based upon varying the radial grid size show the 8th order convergence in the shear expected from the Runge-Kutta integration and splines. When the radial source of error is small, reduced error with smaller time step can also be discerned.

In practical runs, the major source of inaccuracy is the spherical harmonic resolution, currently restricted to $\ell \leq 15$ by hardware limitations. Truncation of the spherical harmonic expansion has the effect of modifying the equations to a system for which the constraints are no longer satisfied. The relative error in the constraints is $10^{-3}$ for strong field simulations [17].

### 3.5.5 Nonlinear Scattering Off a Schwarzschild Black Hole

A natural physical application of a characteristic evolution code is the nonlinear version of the classic problem of scattering off a Schwarzschild black hole, first solved perturbatively by Price [116]. Here the inner worldtube for the characteristic initial value problem consists of the ingoing $r = 2m$ surface (the past horizon), where Schwarzschild data are prescribed. The nonlinear problem of a gravitational wave scattering off a Schwarzschild black hole is then posed in terms of data on an outgoing null cone consisting of an incoming pulse with compact support. Part of the energy of this pulse falls into the black hole and part is backscattered out to $\mathcal{I}^+$. This problem has been investigated using both the PITT and Canberra codes.

The Pittsburgh group studied the backscattered waveform (described by the Bondi news function) as a function of incoming pulse amplitude. The computational eth module smoothly handled the complicated time dependent transformation between the non-inertial computational frame at $\mathcal{I}^+$ and the inertial (Bondi) frame necessary to obtain the standard "plus" and "cross" polarization modes. In the perturbative regime, the news corresponds to the backscattering of the incoming pulse off the effective Schwarzschild potential. When the energy of the pulse is no larger than the central Schwarzschild mass, the backscattered waveform still depends roughly linearly on the amplitude of the incoming pulse. However, for very high amplitudes the waveform behaves quite differently. Its amplitude is greater than that predicted by linear scaling and its shape drasti-

cally changes and exhibits extra oscillations. In this very high amplitude case, the mass of the system is completely dominated by the incoming pulse, which essentially backscatters off itself in a nonlinear way.

The Canberra code was used to study the change in Bondi mass due to radiation [17]. The Hawking mass $M_{\rm H}(u,r)$ is first calculated as a function of radius and retarded time, with the Bondi mass $M_{\rm B}(u)$ then obtained by taking the limit $r \to \infty$. The limit has good numerical behavior. For a strong initial pulse with $\ell = 4$ angular dependence, in a run from $u = 0$ to $u = 70$ (in units where the interior Schwarzschild mass is 1), the Bondi mass drops from 1.8 to 1.00002, showing that almost half of the initial energy of the system was backscattered and that a surprisingly negligible amount falls into the black hole. The Bondi mass decreases monotonically in time, as theoretically necessary, but its rate of change exhibits an interesting pulsing behavior whose time scale cannot be obviously explained in terms of quasinormal oscillations. The Bondi mass loss formula is confirmed with relative error of less than $10^{-3}$. This is impressive accuracy considering the potential sources of numerical error introduced by taking the limit of the Hawking mass. The Canberra group also studied the effect of initial pulse amplitude on the waveform of the backscattered radiation but did not extend their study to the very high amplitude regime in which qualitatively interesting nonlinear effects occur.

### 3.5.6 Black Hole in a Box

The PITT code has also been implemented to evolve along a family of *ingoing* null cones, with data given on a worldtube at their *outer* boundary and on an initial *ingoing* null cone. The code was used to evolve a black hole in the region interior to the worldtube by locating the marginally trapped surface (MTS) on the ingoing cones and excising its singular interior [73]. The code tracks the motion of the MTS and measures its area during the evolution. It was used to simulate a distorted "black hole in a box" [70]. Data at the outer worldtube was induced from a Schwarzschild or Kerr spacetime but the worldtube was allowed to move relative to the stationary trajectories; i.e. with respect to the grid the worldtube is fixed but the black hole moves inside it. The initial null data consisted of a pulse of radiation which subsequently travels outward to the worldtube where it reflects back toward the black hole. The approach of the system to equilibrium was monitored by the area of the MTS, which also equals its Hawking mass. When the worldtube is stationary (static or rotating in place), the distorted black hole inside evolves to equilibrium with the boundary. A boost or other motion of the worldtube with respect to the black hole does not affect this result. The marginally trapped surface always reaches equilibrium with the outer boundary, confirming that the motion of the boundary is "pure gauge".

The code essentially runs "forever" even when the worldtube wobbles with respect to the black hole to produce artificial periodic time dependence. An initially distorted, wobbling black hole was evolved for a time of 60,000 $M$, longer by orders of magnitude than stability permits for any other existing 3D

black hole code. This exceptional performance opens a promising new approach to handle the inner boundary condition for Cauchy evolution of black holes by the matching methods reviewed in Sec. 4.

### 3.6 Characteristic Treatment of Binary Black Holes

An important application of characteristic evolution is the calculation of the waveform emitted by binary black holes, which is possible during the very interesting nonlinear domain from merger to ringdown [100, 154]. The evolution is carried out along a family of ingoing null hypersurfaces which intersect the horizon in topological spheres. It is restricted to the period following the merger, for otherwise the ingoing null hypersurfaces would intersect the horizon in disjoint pieces corresponding to the individual black holes. The evolution proceeds *backward* in time on an ingoing null foliation to determine the exterior spacetime in the post-merger era. It is an example of the characteristic initial value problem posed on an intersecting pair of null hypersurfaces [123, 85], for which existence theorems apply in some neighborhood of the initial null hypersurfaces [157, 60, 59]. Here one of the null hypersurfaces is the event horizon $\mathcal{H}$ of the binary black holes. The other is an ingoing null hypersurface $J^+$ which intersects $\mathcal{H}$ in a topologically spherical surface $\mathcal{S}^+$ approximating the equilibrium of the final Kerr black hole, so that $J^+$ approximates future null infinity $\mathcal{I}^+$. The required data for the analytic problem consists of the degenerate conformal null metrics of $\mathcal{H}$ and $J^+$ and the metric and extrinsic curvature of $\mathcal{S}^+$.

The conformal metric of $\mathcal{H}$ is provided by the conformal horizon model for a binary black hole horizon [100, 89], which treats the horizon in stand-alone fashion as a three-dimensional manifold endowed with a degenerate metric $\gamma_{ab}$ and affine parameter $t$ along its null rays. The metric is obtained from the conformal mapping $\gamma_{ab} = \Omega^2 \hat{\gamma}_{ab}$ of the intrinsic metric $\hat{\gamma}_{ab}$ of a flat space null hypersurface emanating from a convex surface $\mathcal{S}_0$ embedded at constant time in Minkowski space. The horizon is identified with the null hypersurface formed by the inner branch of the boundary of the past of $\mathcal{S}_0$, and its extension into the future. The flat space null hypersurface expands forever as its affine parameter $\hat{t}$ (given by Minkowski time) increases but the conformal factor is chosen to stop the expansion so that the cross-sectional area of the black hole approaches a finite limit in the future. At the same time, the Raychaudhuri equation (which governs the growth of surface area) forces a nonlinear relation between the affine parameters $t$ and $\hat{t}$ which produces the nontrivial topology of the affine slices of the black hole horizon. The relative distortion between the affine parameters $t$ and $\hat{t}$, brought about by curved space focusing, gives rise to the trousers shape of a binary black hole horizon.

An embedding diagram of the horizon for an axisymmetric head-on collision, obtained by choosing $\mathcal{S}_0$ to be a prolate spheroid, is shown in Fig. 3 [100]. The black hole event horizon associated with a triaxial ellipsoid reveals new features not seen in the degenerate case of the head-on collision [89], as depicted in Fig. 4. If the degeneracy is slightly broken, the individual black holes form with spherical topology but as they approach, tidal distortion produces two sharp

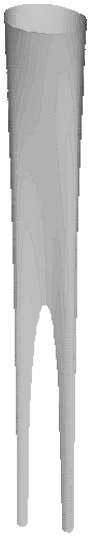

Figure 3: *Trousers shaped event horizon obtained by the conformal model.*

pincers on each black hole just prior to merger. At merger, the two pincers join to form a single temporarily toroidal black hole. The inner hole of the torus subsequently closes up (superluminally) to produce first a peanut shaped black hole and finally a spherical black hole. In the degenerate axisymmetric limit, the pincers reduce to a point so that the individual holes have teardrop shape and they merge without a toroidal phase. No violation of the topological censorship [58] occurs because the hole in the torus closes up superluminally. Consequently, a causal curve passing through the torus at a given time can be slipped below the bottom of a trouser leg to yield a causal curve lying entirely outside the hole [126]. Details of this merger can be viewed at [150].

The conformal horizon model determines the data on $\mathcal{H}$ and $\mathcal{S}^+$. The remaining data necessary to evolve the exterior spacetime is the conformal geometry of $J^+$, which constitutes the outgoing radiation waveform. The determination of the merger-ringdown waveform proceeds in two stages. In the first stage, this outgoing waveform is set to zero and the spacetime is evolved backward in time to calculate the incoming radiation entering from $\mathcal{I}^-$. (This incoming radiation is eventually absorbed by the black hole.) From a time reversed point of view, this evolution describes the outgoing waveform emitted in the fission of a white hole, with the physically correct initial condition of no ingoing radiation. Preliminary calculations show that at late times the waveform is entirely quadrupole ($\ell = 2$) but that a strong $\ell = 4$ mode exists just before fission. In the second stage of the calculation, which has not yet been carried out, this waveform is used to generate the physically correct outgoing waveform for a black hole merger. The passage from the first stage to the second is the nonlinear equivalent of first determining an inhomogeneous solution to a linear problem

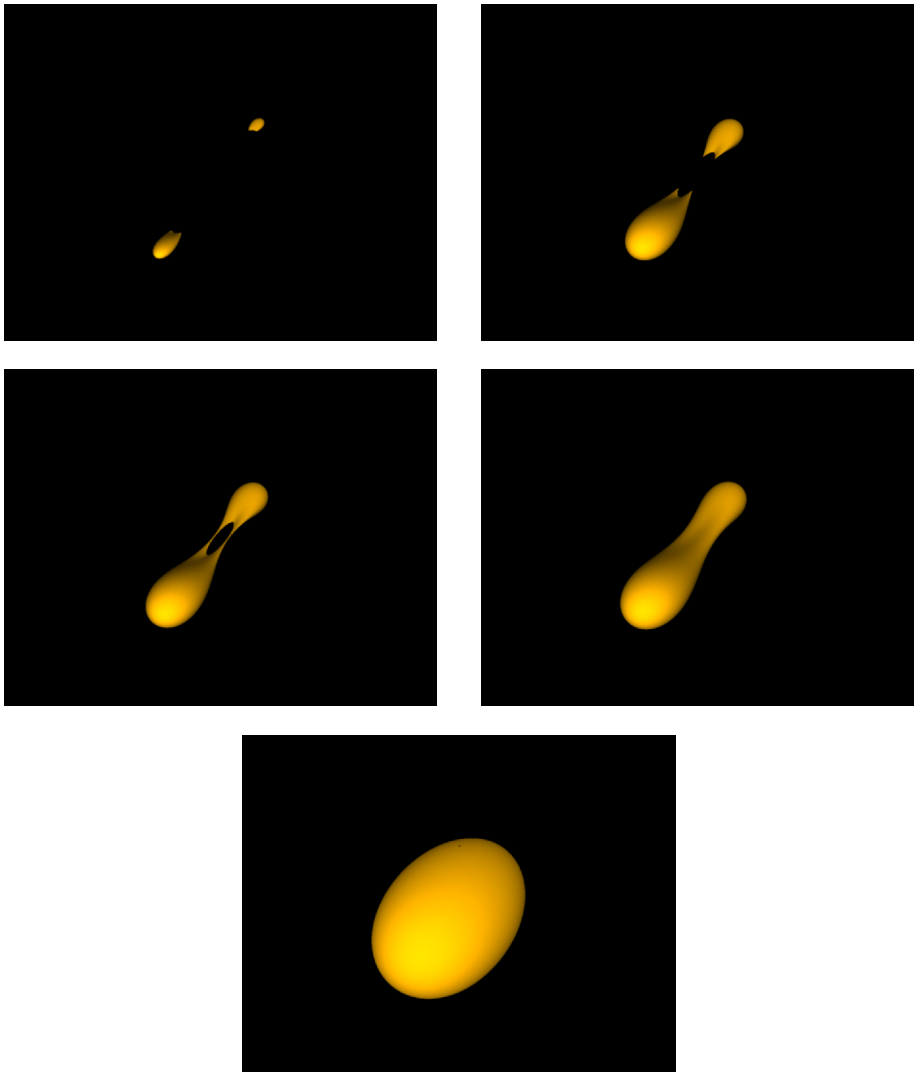

Figure 4: *Upper left panel: Tidal distortion of approaching black holes. Upper right panel: Formation of sharp pincers just prior to merger. Middle left panel: Temporarily toroidal stage just after merger. Middle right panel: Peanut shape black hole after the hole in the torus closes. Lower panel: Approach to final equilibrium.*

and then adding the appropriate homogeneous solution to satisfy the boundary conditions. In this context, the first stage supplies an advanced solution and the second stage the homogeneous retarded minus advanced solution. When the evolution is carried out in the perturbative regime of a Kerr or Schwarzschild background, as in the close approximation [117], this superposition of solutions is simplified by the time reflection symmetry [154]. More generally, beyond the perturbative regime, the merger-ringdown waveform must be obtained by a more complicated inverse scattering procedure.

There is a complication in applying the PITT code to this double null evolution because a dynamic horizon does not lie precisely on $r$-grid points. As a result, the $r$-derivative of the null data, i.e. the ingoing shear of $\mathcal{H}$, must also be provided in order to initiate the radial hypersurface integrations. The ingoing shear is part of the free data specified at $\mathcal{S}^+$. Its value on $\mathcal{H}$ can be determined by integrating (backward in time) a sequence of propagation equations involving the horizon's twist and ingoing divergence. A horizon code which carries out these integrations has been tested to give accurate data even beyond the merger [68].

The code has revealed new global properties of the head-on collision by studying a sequence of data for a family of colliding black holes which approaches a single Schwarzschild black hole. The resulting perturbed Schwarzschild horizon provides global insight into the close limit [117], in which the individual black holes have joined in the infinite past. A marginally anti-trapped surface divides the horizon into interior and exterior regions, analogous to the division of the Schwarzschild horizon by the $r = 2M$ bifurcation sphere. In passing from the perturbative to the strongly nonlinear regime there is a rapid transition in which the individual black holes move into the exterior portion of the horizon. The data paves the way for the PITT code to calculate whether this dramatic time dependence of the horizon produces an equally dramatic waveform.

# 4 Cauchy-Characteristic Matching

Characteristic evolution has many advantages over Cauchy evolution. Its one disadvantage is the existence of either caustics where neighboring characteristics focus or, a milder version consisting of crossover between two distinct characteristics. The vertex of a light cone is a highly symmetric caustic which already strongly limits the time step for characteristic evolution because of the CFL condition. It does not seem possible for a single characteristic coordinate system to cover the entire exterior region of a binary black hole spacetime without developing more complicated caustics or crossovers. This limits the waveform determined by a purely characteristic evolution to the post merger period.

Cauchy-characteristic matching (CCM) is a way to avoid such limitations by combining the strong points of characteristic and Cauchy evolution into a global evolution [25]. One of the prime goals of computational relativity is the simulation of the inspiral and merger of binary black holes. Given the appropriate worldtube data for a binary system in its interior, characteristic evolution can supply the exterior spacetime and the radiated waveform. But determination of the worldtube data for a binary requires an interior Cauchy evolution. CCM is designed to solve such global problems. The potential advantages of CCM over traditional boundary conditions are:

1. accurate waveform and polarization properties at infinity,

2. computational efficiency for radiation problems in terms of both the grid domain and the computational algorithm,

3. elimination of an artificial outer boundary condition on the Cauchy problem, which eliminates contamination from back reflection and clarifies the global initial value problem, and

4. a global picture of the spacetime exterior to the horizon.

These advantages have been realized in model tests but CCM has not yet been successful in either axisymmetric or fully three-dimensional general relativity. This difficulty may possibly arise from a pathology in the way boundary conditions have traditionally been applied in the Arnowitt-Deser-Misner (ADM) [10] formulation of the Einstein equations which, at present, is the only formulation for which CCM has been attempted.

Instabilities or inaccuracies introduced at boundaries have emerged as a major problem common to all ADM code development and have led to pessimism that such codes might be inherently unstable because of the lack of manifest hyperbolicity in the underlying equations. In order to shed light on this issue, B. Szilágyi [137, 138], as part of his thesis research, carried out a study of ADM evolution-boundary algorithms in the simple environment of linearized gravity, where nonlinear sources of physical or numerical instability are absent and computing time is reduced by a factor of five by use of a linearized code. The two main results, for prescribed values of lapse and shift, were:

- On analytic grounds, ADM boundary algorithms which supply values for all components of the metric (or extrinsic curvature) are inconsistent.

- Using a consistent boundary algorithm, which only allows free specification of the transverse-traceless components of the metric with respect to the boundary, an unconstrained, linearized ADM evolution can be carried out in a bounded domain for thousands of crossing times with robust stability.

The criteria for robust stability is that the initial Cauchy data and free boundary data be prescribed as random numbers. It is the most severe test of stability yet carried out in the Cauchy evolution of general relativity. Similar robust stability tests were previously successfully carried out for the PITT characteristic code.

CCM cannot work unless the Cauchy code, as well as the characteristic code, has a robustly stable boundary. This is necessarily so because interpolations continually introduce short wavelength noise into the neighborhood of the boundary. Robustness of the Cauchy boundary is a necessary (although not a sufficient) condition for the successful implementation of CCM. The robustly stable ADM evolution-boundary algorithm differs from previous approaches and offers fresh hope for the success of CCM in general relativity.

## 4.1 Computational Boundaries

Boundary conditions are both the most important and the most difficult part of a theoretical treatment of most physical systems. Usually, that's where all the physics is. And, in computational approaches, that's usually where all the agony is. Computational boundaries for hyperbolic systems pose special difficulties. Even with an analytic form of the correct physical boundary condition in hand, there are seemingly infinitely more unstable numerical implementations than stable ones. In general, a well posed problem places more boundary requirements on the finite difference equations than on the corresponding partial differential equations. Furthermore, the methods of linear stability analysis are often more unwieldy to apply to the boundary than to the interior evolution algorithm.

The von Neumann stability analysis of the interior algorithm linearizes the equations, while assuming a uniform infinite grid, and checks that the discrete Fourier modes do not grow exponentially. There is an additional stability condition that a boundary introduces into this analysis. Consider the one-dimensional case. Normally the mode $e^{kx}$, with $k$ real, is not included in the von Neumann analysis. However, if there is a boundary to the right on the $x$-axis, one can legitimately prescribe such a mode (with $k > 0$) as initial data, so that its stability must be checked. In the case of an additional boundary to the left, the Ryaben'kii-Godunov theory allows separate investigation of the interior stability and the stability of each individual boundary [128].

The correct physical formulation of any asymptotically flat, radiative Cauchy problem also requires boundary conditions at infinity. These conditions must

ensure not only that the total energy and the energy loss by radiation are both finite, but must also ensure the proper $1/r$ asymptotic falloff of the radiation fields. However, when treating radiative systems computationally, an outer boundary must be established artificially at some large but finite distance in the wave zone, i.e. many wavelengths from the source. Imposing an accurate radiation boundary condition at a finite distance is a difficult task even in the case of a simple radiative system evolving on a fixed geometric background. The problem is exacerbated when dealing with Einstein's equation.

Nowhere is the boundary problem more acute than in the computation of gravitational radiation produced by black holes. The numerical study of a black hole spacetime by means of a pure Cauchy evolution involves inner as well as outer grid boundaries. The inner boundary is necessary to avoid the topological complications and singularities introduced by a black hole. For multiple black holes, the inner boundary consists of disjoint pieces. W. Unruh (see [145]) initially suggested the commonly accepted strategy for Cauchy evolution of black holes. An inner boundary located at (or near) an apparent horizon is used to excise the singular interior region. Later (see Sec. 4.8) I discuss a variation of this strategy based upon matching to a characteristic evolution in the inner region.

First, consider the outer boundary problem, in which Cauchy-characteristic matching has a natural application. In the Cauchy treatment of such a system, the outer grid boundary is located at some finite distance, normally many wavelengths from the source. Attempts to use compactified Cauchy hypersurfaces which extend to spatial infinity have failed because the phase of short wavelength radiation varies rapidly in spatial directions [93]. Characteristic evolution avoids this problem by approaching infinity along phase fronts.

When the system is nonlinear and not amenable to an exact solution, a finite outer boundary condition must necessarily introduce spurious physical effects into a Cauchy evolution. The domain of dependence of the initial Cauchy data in the region spanned by the computational grid would shrink in time along ingoing characteristics unless data on a worldtube traced out by the outer grid boundary is included as part of the problem. In order to maintain a causally sensible evolution, this worldtube data must correctly substitute for the missing Cauchy data which would have been supplied if the Cauchy hypersurface had extended to infinity. In a scattering problem, this missing exterior Cauchy data might, for instance, correspond to an incoming pulse initially outside the outer boundary. In a problem where the initial radiation fields are confined to a compact region inside the boundary, this missing Cauchy data are easy to state when dealing with a constraint free field, such as a scalar field $\Phi$ where the Cauchy data outside the boundary would be $\Phi_{,t} = 0$. However, the determination of Cauchy data for general relativity is a global elliptic constraint problem so that there is no well defined scheme to confine it to a compact region. Furthermore, even if the data were known on a complete initial hypersurface extending to infinity, it would be a formidable nonlinear problem to correctly pose the associated data on the outer boundary. The only formulation of Einstein's equations whose Cauchy initial-boundary value problem has been shown to have a unique solution is a

symmetric hyperbolic formulation due to Friedrich and Nagy [61]. However, their mathematical treatment does not suggest how to construct a consistent evolution algorithm.

It is common practice in computational physics to impose some artificial boundary condition (ABC), such as an outgoing radiation condition, in an attempt to approximate the proper data for the exterior region. This ABC may cause partial reflection of an outgoing wave back into the system [101, 93, 87, 118], which contaminates the accuracy of the interior evolution and the calculation of the radiated waveform. Furthermore, nonlinear waves intrinsically backscatter, which makes it incorrect to try to entirely eliminate incoming radiation from the outer region. The errors introduced by these problems are of an analytic origin, essentially independent of computational discretization. In general, a systematic reduction of this error can only be achieved by simultaneously refining the discretization and moving the computational boundary to larger and larger radii. This is computationally very expensive, especially for three-dimensional simulations.

A traditional outer boundary condition for the wave equation is the Sommerfeld condition. For a 3D scalar field this takes the form $g_{,t} + g_{,r} = 0$, where $g = r\Phi$. This condition is *exact* for a linear wave with spherically symmetric data and boundary. In that case, the exact solution is $g = f_1(t-r) + f_2(t+r)$ and the Sommerfeld condition eliminates the incoming wave $f_2$.

Much work has been done on formulating boundary conditions, both exact and approximate, for linear problems in situations that are not spherically symmetric and in which the Sommerfeld condition would be inaccurate. These boundary conditions are given various names in the literature, e.g. absorbing or non-reflecting. A variety of successful implementations of ABC's have been reported for linear problems. See the recent articles [66, 118, 148, 120, 27] for a general discussion of ABC's.

Local ABC's have been extensively applied to linear problems with varying success [101, 56, 22, 147, 87, 33, 94]. Some of these conditions are local approximations to exact integral representations of the solution in the exterior of the computational domain [56], while others are based on approximating the dispersion relation of the so-called one-way wave equations [101, 147]. Higdon [87] showed that this last approach is essentially equivalent to specifying a finite number of angles of incidence for which the ABC's yield perfect transmission. Local ABC's have also been derived for the linear wave equation by considering the asymptotic behavior of outgoing solutions [22], which generalizes the Sommerfeld outgoing radiation condition. Although such ABC's are relatively simple to implement and have a low computational cost, their final accuracy is often limited because the assumptions made about the behavior of the waves are rarely met in practice [66, 148].

The disadvantages of local ABC's have led some workers to consider exact nonlocal boundary conditions based on integral representations of the infinite domain problem [146, 66, 148]. Even for problems where the Green's function is known and easily computed, such approaches were initially dismissed as impractical [56]; however, the rapid increase in computer power has made it possible

to implement exact nonlocal ABC's for the linear wave equation and Maxwell's equations in 3D [48, 78]. If properly implemented, this kind of method can yield numerical solutions which converge to the exact infinite domain problem in the continuum limit, keeping the artificial boundary at a fixed distance. However, due to nonlocality, the computational cost per time step usually grows at a higher power with grid size ($O(N^4)$ per time step in three dimensions) than in a local approach [66, 48, 148].

The extension of ABC's to *nonlinear* problems is much more difficult. The problem is normally treated by linearizing the region between the outer boundary and infinity, using either local or nonlocal linear ABC's [148, 120]. The neglect of the nonlinear terms in this region introduces an unavoidable error at the analytic level. But even larger errors are typically introduced in prescribing the outer boundary data. This is a subtle global problem because the correct boundary data must correspond to the continuity of fields and their normal derivatives when extended across the boundary into the linearized exterior. This is a clear requirement for any consistent boundary algorithm, since discontinuities in the field or its derivatives would otherwise act as spurious sheet source on the boundary, thereby contaminating both the interior and the exterior evolutions. But the fields and their normal derivatives constitute an overdetermined set of data for the linearized exterior problem. So it is necessary to solve a global linearized problem, not just an exterior one, in order to find the proper data. The designation "exact ABC" is given to an ABC for a nonlinear system whose only error is due to linearization of the exterior. An exact ABC requires the use of global techniques, such as the difference potential method, to eliminate back reflection at the boundary [148].

To date there have been only a few applications of ABC's to strongly nonlinear problems [66]. Thompson [144] generalized a previous nonlinear ABC of Hedstrom [86] to treat 1D and 2D problems in gas dynamics. These boundary conditions performed poorly in some situations because of their difficulty in adequately modeling the field outside the computational domain [144, 66]. Hagstrom and Hariharan [82] have overcome these difficulties in 1D gas dynamics by a clever use of Riemann invariants. They proposed a heuristic generalization of their local ABC to 3D, but this has not yet been implemented.

In order to reduce the level of approximation at the analytic level, an artificial boundary for an nonlinear problem must be placed sufficiently far from the strong-field region. This sharply increases the computational cost in multidimensional simulations [56]. There seems to be no numerical method which converges (as the discretization is refined) to the infinite domain exact solution of a strongly nonlinear wave problem in multidimensions, while keeping the artificial boundary fixed.

Cauchy-characteristic matching is a strategy that eliminates this nonlinear source of error. In CCM, Cauchy and characteristic evolution algorithms are pasted together in the neighborhood of a worldtube to form a global evolution algorithm. The characteristic algorithm provides an *outer* boundary condition for the interior Cauchy evolution, while the Cauchy algorithm supplies an *inner* boundary condition for the characteristic evolution. The matching worldtube

provides the geometric framework necessary to relate the two evolutions. The Cauchy foliation slices the worldtube into spherical cross-sections. The characteristic evolution is based upon the outgoing null hypersurfaces emanating from these slices, with the evolution proceeding from one hypersurface to the next by the outward radial march described earlier. There is no need to truncate spacetime at a finite distance from the sources, since compactification of the radial null coordinate makes it possible to cover the infinite space with a finite computational grid. In this way, the true waveform may be directly computed by a finite difference algorithm. Although characteristic evolution has limitations in regions where caustics develop, it proves to be both accurate and computationally efficient in the treatment of exterior regions.

CCM evolves a mixed spacelike-null initial value problem in which Cauchy data is given in a spacelike region bounded by a spherical boundary $\mathcal{S}$ and characteristic data is given on a null hypersurface emanating from $\mathcal{S}$. The general idea is not entirely new. An early mathematical investigation combining spacelike and characteristic hypersurfaces appears in the work of Duff [55]. The three chief ingredients for computational implementation are: (i) a Cauchy evolution module, (ii) a characteristic evolution module and (iii) a module for matching the Cauchy and characteristic regions across an interface. The interface is the timelike worldtube which is traced out by the flow of $\mathcal{S}$ along the worldlines of the Cauchy evolution, as determined by the choice of lapse and shift. Matching provides the exchange of data across the worldtube to allow evolution without any further boundary conditions, as would be necessary in either a purely Cauchy or a purely characteristic evolution.

CCM may be formulated as a purely analytic approach, but its advantages are paramount in the solution of nonlinear problems where analytic solutions would be impossible. One of the first applications of CCM was a hybrid numerical-analytical version, initiated by Anderson and Hobill for the 1D wave equation [5] (see below). There the characteristic region was restricted to the far field where it was handled analytically by a linear approximation.

The full potential of CCM lies in a purely numerical treatment of nonlinear systems where its error converges to zero in the continuum limit of infinite grid resolution [24, 25, 45]. For high accuracy, CCM is also by far the most efficient method. For small target error $\varepsilon$, it has been shown that the relative amount of computation required for CCM ($A_{\rm CCM}$) compared to that required for a pure Cauchy calculation ($A_{\rm C}$) goes to zero, $A_{\rm CCM}/A_{\rm C} \to O$ as $\varepsilon \to O$ [31, 28]. An important factor here is the use of a compactified characteristic evolution, so that the whole spacetime is represented on a finite grid. From a numerical point of view this means that the only error made in a calculation of the radiation waveform at infinity is the controlled error due to the finite discretization. Accuracy of a Cauchy algorithm which uses an ABC requires a large grid domain in order to avoid error from nonlinear effects in the exterior. The computational demands of matching are small because the interface problem involves one less dimension than the evolution problem. Because characteristic evolution algorithms are more efficient than Cauchy algorithms, the efficiency can be further enhanced by making the matching radius as small as consistent with avoiding

caustics.

At present, the purely computational version of CCM is exclusively the tool of general relativists who are used to dealing with novel coordinate systems. A discussion of its potential appears in [24]. Only recently [45, 46, 54, 26] has its practicability been carefully explored. Research on this topic has been stimulated by the requirements of the Binary Black Hole Grand Challenge Alliance, where CCM was one of the strategies being pursued to provide the boundary conditions and determine the radiation waveform. But I anticipate that its use will eventually spread throughout computational physics because of its inherent advantages in dealing with hyperbolic systems, particularly in three-dimensional problems where efficiency is desired. A detailed study of the stability and accuracy of CCM for linear and non-linear wave equations has been presented in Ref. [27], illustrating its potential for a wide range of problems.

## 4.2 Perturbative Cauchy-Characteristic Matching

In numerous purely analytic applications outside of general relativity, matching techniques have successfully cured pathologies in perturbative expansions [105]. Matching is a strategy for obtaining a global solution by patching together solutions obtained using different coordinate systems for different regions. By adopting each coordinate system to a length scale appropriate to its domain, a globally convergent perturbation expansion is sometimes possible in cases where a single coordinate system would fail. Burke showed that matching could be used to eliminate some of the divergences arising in perturbative calculations of gravitational radiation [36]. Kates and Kegles further showed that the use of a null coordinate system for the exterior region is essential in perturbation expansions of curved space radiation fields [95]. They investigated the perturbative description of a scalar field on a Schwarzschild background, in which case the asymptotic behavior of the Schwarzschild light cones differs drastically from that of the artificial Minkowski light cones used in the perturbative expansions based upon the flat space Green function. Use of the Minkowski light cones leads to *nonuniformities* in the expansion of the radiation fields which are eliminated by the use of exterior coordinates based upon the true light cones. Kates, Anderson, Kegles and Madonna extended this work to the fully general relativistic case and reached the same conclusion [8].

Anderson later applied this approach to the slow motion approximation of a binary system and obtained a derivation of the radiation reaction effect on the orbital period which avoided some objections to earlier approaches [4]. The use of the true light cones was also essential in formulating a mathematical theorem that the Bondi news function satisfies the Einstein quadrupole formula to leading order in a Newtonian limit [153]. Although questions of mathematical consistency still remain in the perturbative treatment of gravitational radiation, it is clear that the use of characteristic methods pushes these problems to a higher perturbative order. Characteristic techniques are used in present day codes for the Zerilli equation [102].

### 4.3 Analytic-Numerical Matching for Waves

One of the earliest computational applications of null coordinates in a matching scheme was a hybrid numerical-analytical version, by Anderson and Hobill, for the test problem of 1D scalar waves [5, 6, 7]. Although the nonlinear near field cannot be treated analytically in a general relativistic radiation problem, the far field can be handled by a perturbative expansion. Their strategy was to match an inner numerical solution to an approximate outer analytic solution.

The initial conditions for the exterior solution were fixed by requiring that the interior sources be stationary prior to some fixed time. As a result, the exterior analytic solution is causal in the sense that it is stationary in the past of some null cone. This effectively introduces a condition that eliminates extraneous incoming radiation from the system in a physically plausible way and determines the exterior solution uniquely. An overlap region was introduced between the numerical interior and the analytic exterior. In the overlap, the numerical solution was matched to the causal analytic solution, resulting in an evolution that was everywhere causally meaningful.

This is the physically correct approach to a system which is stationary prior to a fixed time but is nontrivial to generalize, say, to the problem of radiation from an orbiting binary. Anderson and Hobill first tackled the 1D model problem of an oscillator coupled to a spherically symmetric, flat space, massless scalar field. The numerical results were in excellent agreement with the exact analytic solution (which could be obtained globally for this problem).

They extended the model to include spherical scalar waves propagating in a spherically symmetric curved background. This introduces backscattering which obscures the concept of a purely outgoing wave. No exact solution exists to this problem so that an approximation method was necessary to determine the exterior analytic solution. The approximation was based upon an expansion parameter controlling the amount of backscatter. In the 0th approximation, the scale parameter vanishes and the problem reduces to the flat space case which can be solved exactly. The flat space Green function was then used to generate higher order corrections.

A key ingredient of this perturbative scheme is that the wave equation is solved in retarded null coordinates $(u, r)$ for the curved space metric, so that the proper causality is built into the Green function at each order of approximation. The transformation from null coordinates $(u, r)$ to Cauchy coordinates $(t, r)$ is known analytically for this problem. This allows a simple match between the null and Cauchy solutions at the boundary of the Cauchy grid. Their scheme is efficient and leads to consistent results in the region that the numerical and analytic solutions overlap. It is capable of handling both strong fields and fast motions.

Later, a global, characteristic, numerical study of the self-gravitating version of this problem, by Gómez and Winicour, confirmed that the use of the true null cones is essential in getting the correct radiated waveform [77]. For quasi-periodic radiation, the phase of the waveform is particular sensitive to the truncation of the outer region at a finite boundary. Although a perturbative

estimate would indicate an $O(M/R)$ error, this error accumulates over many cycles to produce an error of order $\pi$ in the phase.

Anderson and Hobill proposed that their method be extended to general relativity by matching a numerical solution to an analytic $1/r$ expansion in null coordinates. However, the only analytic-numerical matching schemes that have been implemented in general relativity have been based upon perturbations of a Schwarzschild background using the standard Schwarzschild time slicing [1, 3, 2, 142]. It would be interesting to compare results with an analytic-numeric matching scheme based upon the true null cones. However the original proposal by Anderson and Hobill has not been carried out.

## 4.4 Numerical Matching for 1D Gravitational Systems

The first numerical implementations of CCM were 1D feasibility studies. These model problems provided a controlled environment for the development of CCM, in which either exact or independent numerical solutions were known. The following studies showed that CCM worked like a charm in a variety of 1D applications – the matched evolutions were essentially transparent to the presence of the interface.

### 4.4.1 Cylindrical Matching

The Southampton group chose cylindrically symmetric systems as their model problem for developing matching techniques. In preliminary work, they showed how CCM could be consistently carried out for a scalar wave evolving in Minkowski spacetime but expressed in a nontrivial cylindrical coordinate system [45].

They then tackled the gravitational problem. They first set up the machinery necessary for investigating cylindrically symmetric vacuum spacetimes [46]. Although the problem involves only one spatial dimension, there are two independent modes of polarization. The Cauchy metric was treated in the Jordan-Ehlers-Kompaneets canonical form, using coordinates $(t, r, \phi, z)$ adapted to the $(\phi, z)$ cylindrical symmetry. The advantage here is that $u = t - r$ is then a null coordinate which can be used for the characteristic evolution. They successfully recast the equations in a suitably regularized form for the compactification of $\mathcal{I}^+$ in terms of the coordinate $y = \sqrt{1/r}$. The simple analytic relationship between Cauchy coordinates $(t, r)$ and characteristic coordinates $(u, y)$ facilitated the translation between Cauchy and characteristic variables on the matching worldtube, given by $r = \text{const.}$.

They next implemented the scheme as a numerical code. The interior Cauchy evolution was carried out using an unconstrained leapfrog scheme. It is notable that they report no problems with instability, which have arisen in other attempts at unconstrained leapfrog evolution in general relativity. The characteristic evolution also used a leapfrog scheme for the evolution between retarded time levels $u$, while numerically integrating the hypersurface equations outward along the characteristics.

The matching interface was located at points common to both the Cauchy and characteristic grids. In order to update these points by Cauchy evolution, it was necessary to obtain field values at the Cauchy "guard" points which lie outside the worldtube in the characteristic region. These values were obtained by interpolation from characteristic grid points (lying on three levels of null hypersurfaces in order to ensure second order accuracy). Similarly, the boundary data for starting up the characteristic integration was obtained by interpolation from Cauchy grid values inside the worldtube.

The matching code was first tested [54] using exact Weber-Wheeler cylindrical waves [152], which come in from $\mathcal{I}^-$, pass through the symmetry axis and expand out to $\mathcal{I}^+$. The numerical errors were oscillatory with low growth rate, and second order convergence was confirmed. Of special importance, little numerical noise was introduced by the interface. Comparisons of CCM were made with Cauchy evolutions using a standard outgoing radiation boundary condition [112]. At high amplitudes the standard condition developed a large error very quickly and was competitive only for weak waves with a large outer boundary. In contrast, the matching code performed well even with a small matching radius. Some interesting simulations were presented in which an outgoing wave in one polarization mode collided with an incoming wave in the other mode, a problem studied earlier by pure Cauchy evolution [114]. The simulations of the collision were qualitatively similar in these two studies.

The Weber-Wheeler waves contain only one gravitational degree of freedom. The code was next tested [51] using exact cylindrically symmetric solutions, due to Piran, Safier and Katz [113], which contain both degrees of freedom. These solutions are singular at $\mathcal{I}^+$ so that the code had to be suitably modified. Relative errors of the various metric quantities were in the range $10^{-4}$ to $10^{-2}$. The convergence rate of the numerical solution starts off as second order but diminishes to first order after long time evolution. However, more recent modifications, made by U. Sperhake, H. Sjödin and J. A. Vickers after these tests, have produced an improved version of the characteristic code (see Sec. 3.1).

### 4.4.2 Spherical Matching

A joint collaboration between groups at Pennsylvania State University and the University of Pittsburgh applied CCM to the Einstein-Klein-Gordon (EKG) system with spherical symmetry [71]. This model problem allowed simulation of black hole formation as well as wave propagation.

The geometrical setup is analogous to the cylindrically symmetric problem. Initial data were specified on the union of a spacelike hypersurface and a null hypersurface. The evolution used a 3-level Cauchy scheme in the interior and a 2-level characteristic evolution in the compactified exterior. A constrained Cauchy evolution was adopted because of its earlier success in accurately simulating scalar wave collapse [39]. Characteristic evolution was based upon the null parallelogram algorithm Eq. (8). The matching between the Cauchy and characteristic foliations was achieved by imposing continuity conditions on the metric, extrinsic curvature and scalar field variables, ensuring smoothness of

fields and their derivatives across the matching interface. The extensive analytical and numerical studies of this system in recent years aided the development of CCM in this non-trivial geometrical setting without exact solutions by providing basic knowledge of the expected physical and geometrical behavior.

The CCM code accurately handled wave propagation and black hole formation for all values of $M/R$ at the matching radius, with no symptoms of instability or back reflection. Second order accuracy was established by checking energy conservation.

### 4.4.3 Excising 1D Black Holes

In further developmental work on the EKG model, the Pittsburgh group used CCM to formulate a new treatment of the inner Cauchy boundary for a black hole spacetime [73]. In the conventional approach, the inner boundary of the Cauchy evolution is located at an apparent horizon, which must lie inside (or on) the event horizon [151], so that truncation of the interior spacetime at the apparent horizon cannot causally affect the gravitational waves radiated to infinity. This is the physical rationale behind the apparent horizon boundary condition. However, instabilities reported with the conventional approach motivated an alternative treatment.

In the CCM strategy, illustrated in Fig. 5, the interior black hole region is evolved using an *ingoing* null algorithm whose inner boundary is a marginally trapped surface, and whose outer boundary lies outside the black hole and forms the inner boundary of a region evolved by the Cauchy algorithm. In turn, the outer boundary of the Cauchy region is handled by matching to an outgoing null evolution extending to $\mathcal{I}^+$. Data are passed between the inner characteristic and central Cauchy regions using a CCM procedure similar to that already described for an outer Cauchy boundary. The main difference is that, whereas the outer Cauchy boundary is matched to an outgoing null hypersurface, the inner Cauchy boundary is matched to an ingoing null hypersurface which enters the event horizon and terminates at a marginally trapped surface.

The translation from an outgoing to an incoming null evolution algorithm can be easily carried out. The substitution $\beta \to \beta + i\pi/2$ in the 3D version of the Bondi metric (Eq. (3)) provides a simple formal recipe for switching from an outgoing to an ingoing null formalism [73].

In order to ensure that trapped surfaces exist on the ingoing null hypersurfaces, initial data were chosen which guarantee black hole formation. Such data can be obtained from initial Cauchy data for a black hole. However, rather than extending the Cauchy hypersurface inward to an apparent horizon, it was truncated sufficiently far outside the apparent horizon to avoid computational problems with the Cauchy evolution. The initial Cauchy data were then extended into the black hole interior as initial null data until a marginally trapped surface is reached. Two ingredients were essential in order to arrange this. First, the inner matching surface must be chosen to be convex, in the sense that its outward null normals uniformly diverge and its inner null normals uniformly converge. (This is trivial to satisfy in the spherically symmetric case.) Given any physi-

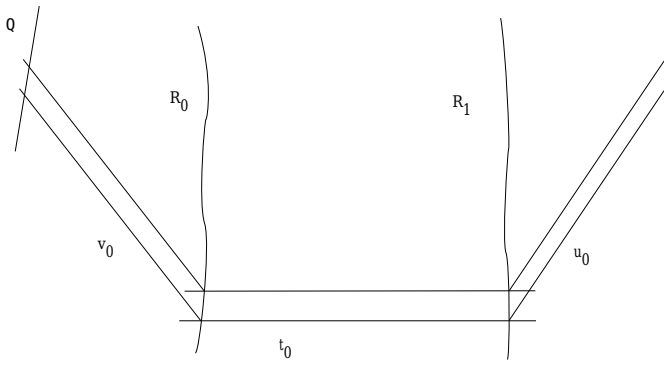


Figure 5: *Black hole excision by matching. A Cauchy evolution, with data at* $t_0$ *is matched across worldtubes* $R_0$ *and* $R_1$ *to an ingoing null evolution, with data at* $v_0$*, and an outgoing null evolution, with data at* $u_0$*. The ingoing null evolution extends to an inner trapped boundary* $Q$*, and the outgoing null evolution extends to* $\mathcal{I}^+$*.*

cally reasonable matter source, the focusing theorem then guarantees that the null rays emanating inward from the matching sphere continue to converge until reaching a caustic. Second, the initial null data must lead to a trapped surface before such a caustic is encountered. This is a relatively easy requirement to satisfy because the initial null data can be posed freely, without any elliptic or algebraic constraints other than continuity with the Cauchy data.

A code was developed which implemented CCM at both the inner and outer boundaries [73]. Its performance showed that CCM provides as good a solution to the black hole excision problem in spherical symmetry as any previous treatment [124, 125, 103, 9]. CCM is computationally more efficient than these pure Cauchy approaches (fewer variables) and much easier to implement. Achieving stability with a pure Cauchy scheme in the region of an apparent horizon is trickier, involving much trial and error in choosing finite difference schemes. There were no complications with stability of the null evolution at the marginally trapped surface.

The Cauchy evolution was carried out in ingoing Eddington-Finklestein (IEF) coordinates. The initial Cauchy data consisted of a Schwarzschild black hole with an ingoing Gaussian pulse of scalar radiation. Since IEF coordinates are based on ingoing null cones, it is possible to construct a simple transformation between the IEF Cauchy metric and the ingoing null metric. Initially there was no scalar field present on either the ingoing or outgoing null patches. The initial values for the Bondi variables $\beta$ and $V$ were determined by matching to the Cauchy data at the matching surfaces and integrating the hypersurface equations (5) and (6).

As the evolution proceeds, the scalar field passes into the black hole, and the marginally trapped surface (MTS) grows outward. The MTS could be easily located in the spherically symmetric case by an algebraic equation. In order

to excise the singular region, the grid points inside the marginally trapped surface were identified and masked out of the evolution. The backscattered radiation propagated cleanly across the outer matching surface to $\mathcal{I}^+$. The strategy worked smoothly, and second order accuracy of the approach was established by comparing it to an independent numerical solution obtained using a second order accurate, purely Cauchy code [103]. As discussed in Sec. 4.8, this inside-outside application of CCM has potential application to the binary black hole problem.

In a variant of this double CCM matching scheme, L. Lehner [99] has eliminated the middle Cauchy region and constructed a 1D code matching the ingoing and outgoing characteristic evolutions directly across a single timelike worldtube. In this way, he is able to simulate the global problem of a scalar wave falling into a black hole by purely characteristic methods.

## 4.5 Axisymmetric Cauchy-Characteristic Matching

The Southampton CCM project is being carried out for spacetimes with (twisting) axial symmetry. The formal basis for the matching scheme was developed by d'Inverno and Vickers [52, 53]. Similar to the Pittsburgh 3D strategy (see Sec. 4.7), matching is based upon an extraction module, which supplies boundary data for the exterior characteristic evolution, and an injection module, which supplies boundary data for the interior Cauchy evolution. However, their use of spherical coordinates for the Cauchy evolution (as opposed to Cartesian coordinates in the 3D strategy) allows use of a matching worldtube $r = R_M$ which lies simultaneously on Cauchy and characteristic gridpoints. This tremendously simplifies the necessary interpolations between the Cauchy and characteristic evolutions, at the expense of dealing with the $r = 0$ coordinate singularity in the Cauchy evolution. The characteristic code (see Sec. 3.3.2) is based upon a compactified Bondi-Sachs formalism. The use of a "radial" Cauchy gauge, in which the Cauchy coordinate $r$ measures the surface area of spheres, simplifies the relation to the Bondi-Sachs coordinates. In the numerical scheme, the metric and its derivatives are passed between the Cauchy and characteristic evolutions exactly at $r = R_M$, thus eliminating the need of a matching interface encompassing a few grid zones, as in the 3D Pittsburgh scheme. This avoids a great deal of interpolation error and computational complexity.

The implementation of the Southampton CCM algorithm into a running code is nearing completion, with preliminary results described by D. Pollney in his thesis [115]. The Cauchy code is based upon the axisymmetric ADM code of Stark and Piran [132] and reproduces their vacuum results for a short time period, after which an instability at the origin becomes manifest. The characteristic code has been tested to reproduce accurately the Schwarzschild and boost-rotation symmetric solutions [23], with more thorough tests of stability and accuracy still being carried out. Much progress has been made but much work remains to make the code useful for scientific application.

### 4.6 Cauchy-Characteristic Matching for 3D Scalar Waves

CCM has been successfully implemented in the fully 3D problem of nonlinear scalar waves evolving in a flat spacetime [27, 26]. This study demonstrated the feasibility of matching between Cartesian Cauchy coordinates and spherical null coordinates, the setup required to apply CCM to the binary black hole problem. Unlike the previous examples of matching, the Cauchy and characteristic patches now did not share a common coordinate which can be used to define the matching interface. This introduced a major complication into the matching procedure, resulting in extensive use of inter-grid interpolation. The accompanying short wavelength numerical noise presented a new challenge in obtaining a stable algorithm.

The nonlinear waves were modeled by the equation

$$c^{-2}\partial_{tt}\Phi = \nabla^2\Phi + F(\Phi) + S(x,y,z,t), \tag{21}$$

with self-coupling $F(\Phi)$ and external source $S$. The initial Cauchy data $\Phi(x,y,z,t_0)$ and $\partial_t\Phi(x,y,z,t_0)$ are assigned in a spatial region bounded by a spherical matching surface of radius $R_{\rm m}$.

The characteristic initial value problem (21) is expressed in standard spherical coordinates $(r,\theta,\varphi)$ and retarded time $u = t - r + R_{\rm m}$:

$$2\partial_{ur}g = \partial_{rr}g - \frac{L^2 g}{r^2} + r(F+S), \tag{22}$$

where $g = r\Phi$ and $L^2$ is the angular momentum operator

$$L^2 g = -\frac{\partial_\theta(\sin\theta\partial_\theta g)}{\sin\theta} - \frac{\partial_{\varphi\varphi}g}{\sin^2\theta}. \tag{23}$$

The initial null data consist of $g(r,\theta,\varphi,u_0)$ on the outgoing characteristic cone $u_0 = t_0$ emanating from the matching worldtube at the initial Cauchy time.

CCM was implemented so that, in the continuum limit, $\Phi$ and its normal derivatives would be continuous across the interface $r = R_{\rm m}$ between the regions of Cauchy and characteristic evolution. The use of a Cartesian discretization in the interior and a spherical discretization in the exterior complicated the treatment of the interface. In particular, the stability of the matching algorithm required careful attention to the details of the inter-grid matching. Nevertheless, there was a reasonably broad range of discretization parameters for which CCM was stable.

Two different ways of handling the spherical coordinates were used. One was based upon two overlapping stereographic grid patches and the other upon a multiquadric approximation using a quasi-regular triangulation of the sphere. Both methods gave similar accuracy. The multiquadric method showed a slightly larger range of stability. Also, two separate tactics were used to implement matching, one based upon straightforward interpolations and the other upon maintaining continuity of derivatives in the outward null direction (a generalization of the Sommerfeld condition). Both methods were stable for a reasonable

range of grid parameters. The solutions were second order accurate and the Richardson extrapolation technique could be used to accelerate convergence.

The performance of CCM was compared to traditional ABC's. As expected, the nonlocal ABC's yielded convergent results only in linear problems, and convergence was not observed for local ABC's, whose restrictive assumptions were violated in all of the numerical experiments. The computational cost of CCM was much lower than that of current nonlocal conditions. In strongly nonlinear problems, matching appears to be the only available method which is able to produce numerical solutions which converge to the exact solution with a fixed boundary.

## 4.7 3D Cauchy-Characteristic Matching

The most important application of CCM is anticipated to be the binary black hole problem. The 3D Cauchy codes now being developed to solve this problem employ a single Cartesian coordinate patch [141]. A thoroughly tested and robust 3D characteristic code is now in place [30], ready to match to the boundaries of this Cauchy patch. Development of a stable implementation of CCM represents the major step necessary to provide a global code for the binary problem.

From a cursory view, the application of CCM to this problem might seem routine, tantamount to translating into finite difference form the textbook construction of an atlas consisting of overlapping coordinate patches. In practice, it is an enormous project.

A CCM module has been constructed and interfaced with Cauchy and characteristic evolution modules. It provides a model of how Cauchy and characteristic codes can be pieced together as modules to form a single global code. The documentation of the underlying geometrical algorithm is given in Ref. [28]. The main submodules of the CCM module are:

- The **outer boundary module** which sets the grid structures. This defines masks identifying which points in the Cauchy grid are to be evolved by the Cauchy module and which points are to be interpolated from the characteristic grid, and vice versa. The reference base for constructing the mask is the matching worldtube, which in Cartesian coordinates is the "Euclidean" sphere $x^2 + y^2 + z^2 = R^2$. The choice of lapse and shift for the Cauchy evolution governs the dynamical and geometrical properties of the matching worldtube.

- The **extraction module** whose input is Cauchy grid data in the neighborhood of the worldtube and whose output is the inner boundary data for the exterior characteristic evolution. This module numerically implements the transformation from Cartesian $\{3 + 1\}$ coordinates to spherical null coordinates. The algorithm makes no perturbative assumptions and is based upon interpolations of the Cauchy data to a set of prescribed points on the worldtube. The metric information is then used to solve for

the null geodesics normal to the slices of the worldtube. This provides the Jacobian for the transformation to null coordinates in the neighborhood of the worldtube. The characteristic evolution module is then used to propagate the data from the worldtube to null infinity, where the waveform is calculated.

- The **injection module** which completes the interface by using the exterior characteristic evolution to supply the outer boundary condition for Cauchy evolution. This is the inverse of the extraction procedure but must be implemented outside the worldtube to allow for overlap between Cauchy and characteristic domains. The overlap region is constructed so that it shrinks to zero in the continuum limit. As a result, the inverse Jacobian can be obtained to prescribed accuracy in terms of an affine parameter expansion of the null geodesics about the worldtube.

The CCM module has been calibrated to give a second order accurate interface between Cauchy and characteristic evolution modules. When its long term stability has been established, it will provide an accurate outer boundary condition for an interior Cauchy evolution by joining it to an exterior characteristic evolution which extracts the waveform at infinity.

## 4.8 The Binary Black Hole Inner Boundary

It is clear that the three-dimensional inspiral and coalescence of black holes challenges the limits of present computational know-how. CCM offers a new approach for excising an interior trapped region which might provide the enhanced flexibility to solve this problem. In a binary system, there are major computational advantages in posing the Cauchy evolution in a frame which is co-rotating with the orbiting black holes. Such a description seems necessary in order to keep the numerical grid from being intrinsically twisted. In this co-orbiting description, the Cauchy evolution requires an inner boundary condition inside the black holes and also an outer boundary condition on a worldtube outside of which the grid rotation is likely to be superluminal. An outgoing characteristic code can routinely handle such superluminal gauge flows in the exterior [30]. Thus, successful implementation of CCM would solve the exterior boundary problem for this co-orbiting description.

CCM also has the potential to handle the two black holes inside the Cauchy region. As described earlier with respect to Fig. 5, an ingoing characteristic code can evolve a moving black hole with long term stability [73, 70]. This means that CCM might also be able to provide the inner boundary condition for Cauchy evolution once stable matching has been accomplished. In this approach, the interior boundary of the Cauchy evolution is located *outside* the apparent horizon and matched to a characteristic evolution based upon ingoing null cones. The inner boundary for the characteristic evolution is a trapped or marginally trapped surface, whose interior is excised from the evolution.

In addition to restricting the Cauchy evolution to the region outside the black holes, this strategy offers several other advantages. Although finding a

marginally trapped surface on the ingoing null hypersurfaces remains an elliptic problem, there is a natural radial coordinate system $(r, \theta, \phi)$ to facilitate its solution. Motion of the black hole through the grid reduces to a one-dimensional radial problem, leaving the angular grid intact and thus reducing the computational complexity of excising the inner singular region. (The angular coordinates can even rotate relative to the Cauchy coordinates in order to accommodate spinning black holes.) The chief danger in this approach is that a caustic might be encountered on the ingoing null hypersurface before entering the trapped region. This is a gauge problem whose solution lies in choosing the right location and geometry of the surface across which the Cauchy and characteristic evolutions are matched. There is a great deal of flexibility here because the characteristic initial data can be posed without constraints.

This global strategy is tailor-made to treat two black holes in the co-orbiting gauge, as illustrated in Fig. 6. Two disjoint characteristic evolutions based upon ingoing null cones are matched across worldtubes to a central Cauchy region. The interior boundary of each of these interior characteristic regions border a trapped surface. At the outer boundary of the Cauchy region, a matched characteristic evolution based upon outgoing null hypersurfaces propagates the radiation to infinity.

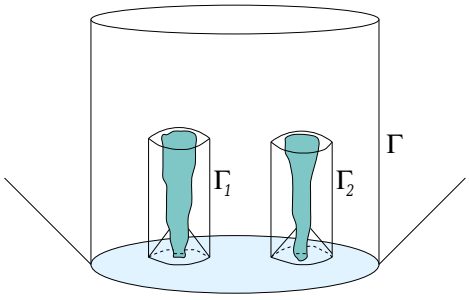


Figure 6: *CCM for binary black holes, portrayed in a co-rotating frame. The Cauchy evolution is matched across two inner worldtubes* $\Gamma_1$ *and* $\Gamma_2$ *to two ingoing null evolutions whose inner boundaries excise the individual black holes. The outer Cauchy boundary is matched across the worldtube* $\Gamma$ *to an outgoing null evolution extending to* $\mathcal{I}^+$.

Present characteristic and Cauchy codes can handle the individual pieces of this problem. Their unification appears to offer the best chance for simulating the inspiral and merger of two black holes. The CCM module is in place and calibrated for accuracy. The one missing ingredient is its long term stability, which would make future reviews of this subject very exciting.

# 5 Numerical Hydrodynamics on Null Cones

Numerical evolution of relativistic hydrodynamics has been traditionally carried out on spacelike Cauchy hypersurfaces. Although the Bondi-Sachs evolution algorithm can easily be extended to include matter [92], the advantage of a light cone approach for treating fluids is not as apparent as for a massless field whose physical characteristics lie on the light cone. However, preliminary results from recent studies of a fluid moving in the vicinity of a black hole indicate that this approach can provide accurate simulations of mass accretion and the gravitational radiation from an infalling body.

In a three-dimensional study, a naive hydrodynamic code for a perfect fluid was incorporated into the PITT null code [29]. The fully nonlinear three-dimensional matter-gravity null code was tested for stability and accuracy to verify that nothing breaks down as long as the fluid remains well behaved, e.g. hydrodynamical shocks do not form. The code was used to simulate a localized blob of matter falling into a black hole, verifying that the motion of the center of the blob approximates a geodesic and determining the waveform of the emitted gravitational radiation at $\mathcal{I}^+$. The results establish the feasibility of a characteristic *matter plus gravity* evolution.

This simulation was a prototype of a neutron star orbiting a black hole. It would be unrealistic to expect that a naive fluid code would allow evolution of a compact star for several orbits as it spiraled into a black hole. However, a refined characteristic hydrodynamic code would open the way to explore this important astrophysical problem. Recently, J. A. Font and P. Papadopoulos [109] successfully implemented such a code in the case of spherical symmetry, using the Bondi-Sachs formalism as adapted to describe gravity coupled to matter inside a worldtube boundary [139].

The approach is based upon a high resolution shock-capturing (HRSC) version of relativistic hydrodynamics developed by the Valencia group (for a review see Ref. [57]). In the HRSC scheme, the hydrodynamic equations are written in flux conservative, hyperbolic form. In each computational cell, the system of equations is diagonalized to determine the characteristic fields and velocities, and the local Riemann problem is solved to obtain a solution consistent with physical discontinuities. This allows a finite differencing scheme along the fluid characteristics that preserves the physically conserved quantities and leads to a stable and accurate treatment of shocks. Because the general relativistic system of hydrodynamical equations is formulated in covariant form, it can equally well be applied to spacelike or null foliations of the spacetime. The null formulation gave remarkable performance in the standard Riemann shock tube test carried out in a Minkowski background and gave second order convergence in curved space tests based upon Tolman-Oppenheimer-Volkoff equilibrium solutions. In the dynamic self-gravitating case, simulations of spherical accretion of a fluid onto a black hole were stable and free of any numerical problems. Accretion was successfully carried out in the regime where the mass of the black hole doubled. In more recent work, they have used the code to study how accretion modulates both decay rates and oscillation frequencies of the quasi-normal modes of the

interior black hole [110].

Plans are being made to combine the characteristic evolution codes for vacuum spacetimes and HRSC relativistic hydrodynamics.

# 6 Acknowledgments

This work was partially supported by NSF PHY 9988663. I want to thank the many people who have supplied me with references. Please keep me updated.

## References

[1] Abrahams, A. M., and Evans, C. R., "Gauge invariant treatment of gravitational radiation near the source: Analysis and numerical spacetimes", *Phys. Rev. D*, **42**(8), 2585–2594, (1990). 1, 4.3

[2] Abrahams, A. M., and Price, R. H., "Applying black hole perturbation theory to numerically generated spacetimes", *Phys. Rev. D*, **53**(4), 1963–1971, (1996). 1, 4.3

[3] Abrahams, A. M., Shapiro, S. L., and Teukolsky, S. A., "Calculation of gravitational waveforms from black hole collisions: Applying perturbation theory to numerical spacetimes", *Phys. Rev. D*, **51**(8), 4295–4301, (1995). 1, 4.3

[4] Anderson, J. L., "Gravitational radiation damping in systems with compact components", *Phys. Rev. D*, **36**(8), 2301–2313, (1987). 4.2

[5] Anderson, J. L., and Hobill, D., "Matched analytic-numerical solutions of wave equations", in Centrella, J., ed., *Dynamical Spacetimes and Numerical Relativity*, 389–410, (Cambridge University Press, Cambridge, 1986). 4.1, 4.3

[6] Anderson, J. L., and Hobill, D. W., "Mixed analytic-numerical solutions for a simple radiating system", *Gen. Relativ. Gravit.*, **19**(6), 563–580, (1987). 4.3

[7] Anderson, J. L., and Hobill, D. W., "A Study of nonlinear radiation damping by matching analytic and numerical solutions", *J. Comput. Phys.*, **75**(2), 283–299, (1988). 4.3

[8] Anderson, J. L., Kates, R. E., Kegles, L. S., and Madonna, R., "Divergent integrals of post-Newtonian gravity: Nonanalytic terms in the near-zone expansion of a gravitationally radiating system found by matching", *J. Math. Phys.*, **25**(8), 2038–2048, (1982). 4.2

[9] Anninos, P., Daues, G., Masso, J., Seidel, E., and Suen, W.-M., "Horizon boundary condition for black hole spacetimes", *Phys. Rev. D*, **51**(10), 5562–5578, (1995). 4.4.3

[10] Arnowitt, R., Deser, S., and Misner, C. W., "The dynamics of general relativity", in Witten, L., ed., *Gravitation – an introduction to current research*, 227, (Wiley, New York, 1962). 4

[11] Barreto, W., and Da Silva, A., "Gravitational collapse of a charged and radiating fluid ball in the diffusion limit", *Gen. Relativ. Gravit.*, **28**(6), 735–747, (1996). 3.1

[12] Barreto, W., and Da Silva, A., "Self-similar and charged spheres in the diffusion approximation", *Class. Quantum Grav.*, **16**(6), 1783–1792, (1999). 3.1

[13] Barreto, W., Gómez, R., Lehner, L., and Winicour, J., "Gravitational Instability of a Kink", *Phys. Rev. D*, **54**(6), 3834–3839, (1996). 3.1

[14] Barreto, W., Peralta, C., and Rosales, R., "Equation of state and transport processes in self-similar spheres", *Phys. Rev. D*, **59**, 024008, (1998). 3.1

[15] Bartnik, R., "Einstein equations in the null quasi-spherical gauge", *Class. Quantum Grav.*, **14**(8), 2185–2194, (1997). 3.5.1

[16] Bartnik, R., "Shear-free null quasi-spherical spacetimes", *J. Math. Phys.*, **38**(11), 5774–5791, (1997). 3.5.1

[17] Bartnik, R., "Interaction of gravitational waves with a black hole", in Bracken, T., and De-Wit, D., eds., *XIIth Int'l Congress Math. Phys.*, 3, (International Press, Hong Kong, 1999). 3.4, 3.5.4, 3.5.5

[18] Bartnik, R., "Assessing accuracy in a numerical Einstein solver", in Weinstein, G., and Weikard, R., eds., *Differential equations and mathematical physics*, 11, (International Press, Cambridge, 2000). 3.5.3

[19] Bartnik, R., and Norton, A. H., "Numerical solution of the Einstein equations", in Noye, B. J., Teubner, M. D., and Gill, A. W., eds., *Computational Techniques and Applications: CTAC97*, 91, (World Scientific, Singapore, 1998). 3.5.3

[20] Bartnik, R., and Norton, A. H., "Geometric implementation of spherical harmonics", in *Computational Techniques and Applications: CTAC99*, J. Austral. Math. Soc., Series B, (2000). To appear. 3.5.2

[21] Bartnik, R., and Norton, A. H., "Numerical methods for the Einstein equations in null quasi-spherical coordinates", *SIAM J. Sci. Comput.*, **22**(3), 917–950, (2000). 3.4, 3.5.3

[22] Bayliss, A., and Turkel, E., "Radiation boundary conditions for wavelike equations", *Commun. Pure Appl. Math.*, **XXXIII**, 707–725, (1980). 4.1

[23] Bicak, J., Reilly, P., and Winicour, J., "Boost-rotation symmetric gravitational null cone data", *Gen. Relativ. Gravit.*, **20**(2), 171–181, (1988). 3.5.4, 4.5

[24] Bishop, N. T., "Some aspects of the characteristic initial value problem in numerical relativity", in d'Inverno, R., ed., *Approaches to Numerical Relativity*, 20–33, (Cambridge University Press, Cambridge,, 1992). 4.1

[25] Bishop, N. T., "Numerical relativity combining the Cauchy and characteristic initial value problem", *Class. Quantum Grav.*, **10**(2), 333–341, (1993). 4, 4.1

[26] Bishop, N. T., Gómez, R., Holvorcem, P. R., Matzner, R. A., Papadopoulos, P, and Winicour, J., "Cauchy-characteristic matching: A new approach to radiation boundary conditions", *Phys. Rev. Lett.*, **76**(23), 4303–4306, (1996). 4.1, 4.6

[27] Bishop, N. T., Gómez, R., Holvorcem, P. R., Matzner, R. A., Papadopoulos, P, and Winicour, J., "Cauchy-characteristic evolution and waveforms", *J. Comput. Phys.*, **136**(1), 140–167, (1997). 4.1, 4.6

[28] Bishop, N. T., Gómez, R., Isaacson, R. A., Lehner, L., Szilagyi, B., and Winicour, J, "Cauchy Characteristic Matching", in Bhawal, B., and Iyer, B. R., eds., *On the Black Hole Trail*, chapter 24, 383, (Kluwer, Dordrecht, 1998). 4.1, 4.7

[29] Bishop, N. T., Gómez, R., Lehner, L., , Maharaj, M., and Winicour, J., "The incorporation of matter into characteristic numerical relativity", *Phys. Rev. D*, **60**(2), 24005, (1999). 5

[30] Bishop, N. T., Gómez, R., Lehner, L., Maharaj, M., and Winicour, J., "High-powered Gravitational News", *Phys. Rev. D*, **56**(10), 6298–6309, (1997). 3.5, 3.5.3, 3.5.4, 4.7, 4.8

[31] Bishop, N. T., Gómez, R., Lehner, L., and Winicour, J., "Cauchy-characteristic extraction in numerical relativity", *Phys. Rev. D*, **54**(10), 6153–6165, (1996). 3.5, 3.5.1, 3.5.3, 3.5.4, 4.1

[32] Bizoń, P., "Equivariant self-similar wave maps from Minkowski spacetime into 3-sphere", To appear in Commun. Math. Phys. 3.1

[33] Blaschak, J., and Kriegsmann, G., "A comparative study of absorbing boundary conditions", *J. Comput. Phys.*, **77**, 109–139, (1988). 4.1

[34] Bondi, H., "Gravitational waves in general relativity", *Nature*, **186**, 535–535, (1960). 1, 2

[35] Bondi, H., van der Burg, M. J. G., and Metzner, A. W. K., "Gravitational waves in general relativity VII. Waves from axi-symmetric isolated systems", *Proc. R. Soc. London, Ser. A*, **269**, 21–52, (1962). 1, 2, 3.3, 3.3

[36] Burke, W. L., "Gravitational radiation damping of slowly moving systems calculated using matched asymptotic expansions", *J. Math. Phys.*, **12**(3), 401–418, (1971). 4.2

[37] Butler, D. S., "The numerical solution of hyperbolic systems of partial differential equations in three independent variables", *Proc. R. Soc. London, Ser. A*, **255**, 232–252, (1960). 3.2

[38] Choptuik, M. W., "Critical behavior in massless scalar field collapse", in d'Inverno, R., ed., *Approaches to Numerical Relativity*, 202, (Cambridge University Press, Cambridge, 1992). 3.1

[39] Choptuik, M. W., "Universality and scaling in gravitational collapse of a massless scalar field", *Phys. Rev. Lett.*, **70**(1), 9–12, (1993). 3.1, 4.4.2

[40] Christodoulou, D., "Global existence of generalized solutions of the spherically symmetric Einstein-scalar equations in the large", *Commun. Math. Phys.*, **106**(4), 587–621, (1986). 3.1

[41] Christodoulou, D., "The problem of a self-gravitating scalar field", *Commun. Math. Phys.*, **105**(3), 337–361, (1986). 3.1

[42] Christodoulou, D., "A mathematical theory of gravitational collapse", *Commun. Math. Phys.*, **109**(4), 613–647, (1987). 3.1

[43] Christodoulou, D., "The structure and uniqueness of generalized solutions of the spherically symmetric Einstein-scalar equations", *Commun. Math. Phys.*, **109**(4), 591–611, (1987). 3.1

[44] Christodoulou, D., and Klainerman, S., *The Global Nonlinear Stability of the Minkowski Space*, (Princeton University Press, Princeton, 1993). 3.3

[45] Clarke, C., and d'Inverno, R., "Combining Cauchy and characteristic numerical evolutions in curved coordinates", *Class. Quantum Grav.*, **11**(6), 1463–1448, (1994). 4.1, 4.4.1

[46] Clarke, C., d'Inverno, R., and Vickers, J., "Combining Cauchy and characteristic codes. I. The vacuum cylindrically symmetric problem", *Phys. Rev. D*, **52**(12), 6863–6867, (1995). 3.1, 4.1, 4.4.1

[47] Corkill, R. W., and Stewart, J. M., "Numerical relativity II. Numerical methods for the characteristic initial value problem and the evolution of the vacuum field equations for space-times with two Killing vectors", *Proc. R. Soc. London, Ser. A*, **386**, 373–391, (1983). 3, 3.1

[48] de Moerloose, J., and de Zutter, D., "Surface integral representation boundary condition for the FDTD method", *IEEE Trans. Ant. Prop.*, **41**(7), 890–896, (1993). 4.1

[49] Derry, L., Isaacson, R., and Winicour, J., "Shear-Free Gravitational Radiation", *Phys. Rev.*, **185**(5), 1647–1655, (1969). 3.5.1

[50] d'Inverno, R. A., ed., *Approaches to Numerical Relativity*, (Cambridge University Press, Cambridge, 1992). 2

[51] d'Inverno, R. A., Dubal, M. R., and Sarkies, E. A., "Cauchy-characteristic matching for a family of cylindrical vacuum solutions possessing both gravitational degrees of freedom", *Class. Quantum Grav.*, **17**(16), 3157–3170, (2000). 4.4.1

[52] d'Inverno, R. A., and Vickers, J. A., "Combining Cauchy and characteristic codes. III. The interface problem in axial symmetry", *Phys. Rev. D*, **54**(8), 4919–4928, (1996). 3.3.2, 4.5

[53] d'Inverno, R. A., and Vickers, J. A., "Combining Cauchy and characteristic codes. IV. The characteristic field equations in axial symmetry", *Phys. Rev. D*, **56**(2), 772–784, (1997). 3.3.2, 4.5

[54] Dubal, M., d'Inverno, R., and Clarke, C., "Combining Cauchy and characteristic codes. II. The interface problem for vacuum cylindrical symmetry", *Phys. Rev. D*, **52**(12), 6868–6881, (1995). 3.1, 4.1, 4.4.1

[55] Duff, G. F. D., "Mixed problems for linear systems of first order equations", *Can. J. Math.*, **10**, 127, (1958). 4.1

[56] Engquist, B., and Majda, A., "Absorbing boundary conditions for the numerical simulation of waves", *Math. Comput.*, **31**(139), 629–651, (1977). 4.1

[57] Font, J. A., "Numerical hydrodynamics in general relativity", (March, 2000), [Article in Online Journal Living Reviews in Relativity]: cited on 18 January 2001, `http://www.livingreviews.org/Articles/Volume3/2000-2font`. 5

[58] Friedman, J. L., Schleich, K., and Witt, D. M., "Topological censorship", *Phys. Rev. Lett.*, **71**(10), 1486–1489, (1993). 3.6

[59] Friedrich, H., "The asymptotic characteristic initial value problem for Einstein's vacuum field equations as an initial value problem for a first-order quasilinear symmetric hyperbolic system", *Proc. R. Soc. London, Ser. A*, **378**, 401–421, (1981). 3.3.1, 3.6

[60] Friedrich, H., "On the regular and the asymptotic characteristic initial value problem for Einstein's vacuum field equations", *Proc. R. Soc. London, Ser. A*, **375**, 169–184, (1981). 3.6

[61] Friedrich, H., and Nagy, G., "The initial boundary value problem for Einstein's Field equations", *Commun. Math. Phys.*, **201**(3), 619–655, (1999). 4.1

[62] Friedrich, H., and Stewart, J. M., "Characteristic initial data and wavefront singularities in general relativity", *Proc. R. Soc. London, Ser. A*, **385**, 345–371, (1983). 1, 3.3.1

[63] Garfinkel, D., "Choptuik scaling in null coordinates", *Phys. Rev. D*, **51**(10), 5558–5561, (1995). 3.1

[64] Garfinkel, D., Cutler, C., and Duncan, G. C., "Choptuik scaling in six dimensions", *Phys. Rev. D*, **580**, 104007, (1999). 3.1

[65] Geroch, R, "A method for generating solutions of Einstein's equations", *J. Math. Phys.*, **12**(6), 918–924, (1971). 3.1

[66] Givoli, D., "Non-reflecting boundary conditions", *J. Comput. Phys.*, **94**(1), 1–29, (1991). 4.1

[67] Goldwirth, D., and Piran, T., "Gravitational collapse of massless scalar field and cosmic censorship", *Phys. Rev. D*, **36**(12), 3575–3581, (1987). 3.1, 3.5.2

[68] Gómez, R., Husa, S., and Winicour, J., "Complete null data for a black hole collision", (September, 2000), [Online Los Alamos Archive Preprint]: cited on 18 January 2001, `http://xxx.lanl.gov/abs/gr-qc/0009092`. 3.6

[69] Gómez, R., Isaacson, R. A., Reilly, P., and Winicour, J., "Post-Newtonian Behavior of the Bondi Mass", *Phys. Rev. D*, **47**(8), 3292–3302, (1993). 3.4

[70] Gómez, R., L., Lehner, Marsa, R., and Winicour, J., "Moving black holes in 3D", *Phys. Rev. D*, **57**(8), 4778–4788, (1997). 3.5, 3.5.3, 3.5.4, 3.5.6, 4.8

[71] Gómez, R., Laguna, P., Papadopoulos, P., and Winicour, J., "Cauchy-characteristic evolution of Einstein-Klein-Gordon Systems", *Phys. Rev. D*, **54**(8), 4719–4727, (1996). 4.4.2

[72] Gómez, R., Lehner, L., Papadopoulos, P., and Winicour, J., "The eth formalism in numerical relativity", *Class. Quantum Grav.*, **14**(4), 977–990, (1997). 3.5.2

[73] Gómez, R., Marsa, R., and Winicour, J., "Black hole excision with matching", *Phys. Rev. D*, **56**(10), 6310–6319, (1997). 3.5, 3.5.6, 4.4.3, 4.4.3, 4.8

[74] Gómez, R., Papadopoulos, P., and Winicour, J., "Null cone evolution of Axisymmetric Vacuum Spacetimes", *J. Math. Phys.*, **35**(8), 4184–4204, (1994). 1, 3.3, 3.5.3

[75] Gómez, R., Schmidt, B., and Winicour, J., "Newman-Penrose Constants and the Tails of Self Gravitating Waves", *Phys. Rev. D*, **49**(6), 2828–2836, (1994). 3.1

[76] Gómez, R., and Winicour, J., "Asymptotics of Gravitational Collapse of Scalar Waves", *J. Math. Phys.*, **33**(4), 1445–1457, (1992). 3.1, 3.1

[77] Gómez, R., and Winicour, J., "Gravitational wave forms at finite distances and at null infinity", *Phys. Rev. D*, **45**(8), 2776–2782, (1992). 4.3

[78] Grote, M. J., and Keller, J. B.., "Nonreflecting boundary conditions for Maxwell's equations", *J. Comput. Phys.*, **139**(2), 327–342, (1998). 4.1

[79] Gundlach, C., "Critical phenomena in gravitational collapse", (December, 1999), [Article in Online Journal Living Reviews in Relativity]: cited on 18 January 2001, `http://www.livingreviews.org/Articles/Volume2/1999-4gundlach`. 3.1

[80] Gundlach, C., Price, R., and Pullin, J., "Late-time behavior of stellar collapse and explosions: I. Linear Perturbations", *Phys. Rev. D*, **49**(2), 883–889, (1994). 3.1

[81] Gundlach, C., Price, R., and Pullin, J., "Late-time behavior of stellar collapse and explosions: II. Nonlinear Evolution", *Phys. Rev. D*, **49**(2), 890–899, (1994). 3.1

[82] Hagstrom, T. M., and Hariharan, S., "Accurate boundary conditions for exterior problems in gas dynamics", *Math. Comput.*, **51**(184), 581–597, (1988). 4.1

[83] Hamadé, R., Horne, J. H., and Stewart, J. M., "Continuous Self-similarity and $S$-duality", *Class. Quantum Grav.*, **13**, 2241–2253, (1996). 3.1

[84] Hamadé, R., and Stewart, J. M., "The spherically symmetric collapse of a massless scalar field", *Class. Quantum Grav.*, **13**, 497–512, (1996). 3.1

[85] Hayward, S. A., "Dual-null dynamics of the Einstein field", *Class. Quantum Grav.*, **10**(4), 779–790, (1993). 3.6

[86] Hedstrom, G. W., "Nonreflecting boundary conditions for nonlinear hyperbolic systems", *J. Comput. Phys.*, **30**(2), 222–237, (1979). 4.1

[87] Higdon, R., "Absorbing boundary conditions for difference approximations to the multi-dimensional wave equation", *Math. Comput.*, **47**(176), 437–459, (1986). 4.1

[88] Husa, S., Lechner, C., Purrer, M., Thornburg, J., and Aichelburg, P. C., "Type II critical collapse of a self-gravitating nonlinear $\sigma$-model", *Phys. Rev. D*, **62**, 104007, (2000). 3.1

[89] Husa, S., and Winicour, J., "Asymmetric merger of black holes", *Phys. Rev. D*, **60**, 084019, (1999). 3, 3.6, 3.6

[90] Ipser, J., and Horwitz, G., "The problem of maximizing functionals in Newtonian stellar dynamics, and its relation to thermodynamic and dynamical stability", *Astrophys. J.*, **232**(3), 863–873, (1979). 3.1

[91] Isaacson, R. A., Gómez, R., and Winicour, J., "Evolution of Scalar Fields from Characteristic Data", *J. Comput. Phys.*, **98**(1), 11–25, (1992). 1

[92] Isaacson, R. A., Welling, J. S., and Winicour, J., "Null cone computation of gravitational radiation", *J. Math. Phys.*, **24**(7), 1824–1834, (1983). 3.3, 3.3, 3.4, 5

[93] Israeli, M., and Orszag, S. A., "Approximation of radiation boundary conditions", *J. Comput. Phys.*, **41**(1), 115–135, (1981). 4.1

[94] Jiang, H., and Wong, Y. S., "Absorbing boundary conditions for second order hyperbolic equations", *J. Comput. Phys.*, **88**(1), 205–231, (1990). 4.1

[95] Kates, R. E., and Kegeles, L. S., "Nonanalytic terms in the slow-motion expansion of a radiating scalar field on a Schwarzschild background", *Phys. Rev. D*, **25**(8), 2030–2037, (1982). 4.2

[96] Khan, K. A., and Penrose, R., "Scattering of two impulsive gravitational plane waves", *Nature (London)*, **229**, 185–186, (1971). 3.1

[97] Lehner, L.., *Gravitational radiation from black hole spacetimes*, PhD Thesis, (University of Pittsburgh, Pittsburgh, USA, 1998). 1

[98] Lehner, L., "A dissipative algorithm for wave-like equations in the characteristic formulation", *J. Comput. Phys.*, **149**(1), 59–74, (1999). 3.5.3

[99] Lehner, L., "Matching characteristic codes: exploiting two directions general relativity", *Int. J. Mod. Phys. D*, **9**(4), 459–473, (2000). 4.4.3

[100] Lehner, L., Bishop, N. T., Gómez, R., Szilágyi, B., and Winicour, J., "Exact solutions for the intrinsic geometry of black hole coalescence", *Phys. Rev. D*, **60**, 044005, (1999). 3, 3.6, 3.6

[101] Lindman, E., "Free-space boundary conditions for the time dependent wave equation", *J. Comput. Phys.*, **18**(1), 66–78, (1975). 4.1

[102] Lousto, C. H., and Price, R. H., "Understanding initial data for black hole collisions", *Phys. Rev. D*, **56**(10), 6439–6457, (1997). 4.2

[103] Marsa, R. L., and Choptuik, M. W., "Black-hole-scalar-field interactions in spherical symmetry", *Phys. Rev. D*, **54**(8), 4929–4943, (1996). 3.1, 4.4.3

[104] Matzner, R. A., Seidel, H. E., Shapiro, S. L., Smarr, L. L., Suen, W.-M., and Winicour, J., "Geometry of a black hole collision", *Science*, **270**, 941–947, (1995). 3

[105] Nayfeh, A., *Perturbation Methods*, (Wiley, New York, 1973). 4.2

[106] Newman, E. T., and Penrose, R., "An approach to gravitational radiation by a method of spin coefficients", *J. Math. Phys.*, **3**(3), 566–578, (1962). 2

[107] Newman, E. T., and Penrose, R., "Note on the Bondi-Metzner-Sachs group", *J. Math. Phys.*, **7**, 863, (1966). 3.5.2

[108] Newman, E. T., and Penrose, R., "New conservation laws for zero rest-mass fields in asymptotically flat space-time", *Proc. R. Soc. London, Ser. A*, **305**, 175–204, (1968). 3.1

[109] Papadopoulos, P., and Font, J. A., "Relativistic hydrodynamics on spacelike and null surfaces: Formalism and computation of spherically symmetric spacetimes", *Phys. Rev. D*, **61**, 024015, (2000). 5

[110] Papadopoulos, P., and Font, J. A., "Imprints of accretion on gravitational waves from black holes", *Phys. Rev. D*, **63**, 044016, (2001). For a related online version see: P. Papadopoulos, et al., "Imprints of accretion on gravitational waves from black holes", (September, 2000), [Online Los Alamos Archive Preprint]: cited on 18 January 2001, `http://xxx.lanl.gov/abs/gr-qc/0009024`. 5

[111] Penrose, R., "Asymptotic properties of fields and space-times", *Phys. Rev. Lett.*, **10**, 21, (1963). 1, 2

[112] Piran, T., "Numerical codes for cylindrical general relativistic systems", *J. Comput. Phys.*, **35**(2), 254–283, (1980). 4.4.1

[113] Piran, T., Safier, P. N., and Katz, J., "Cylindrical gravitational waves with two degrees of freedom: An exact solution", *Phys. Rev. D*, **34**(2), 331–332, (1986). 4.4.1

[114] Piran, T., Safier, P. N., and Stark, R. N., "General numerical solution of cylindrical gravitational waves", *Phys. Rev. D*, **32**(12), 3101–3107, (1985). 4.4.1

[115] Pollney, D., *Algebraic and numerical techniques in general relativity*, PhD Thesis, (University of Southampton, Southampton, UK, 2000). 1, 3.3.2, 4.5

[116] Price, R. H., "Nonspherical perturbations of relativistic gravitational collapse. I. Scalar and gravitational perturbations", *Phys. Rev. D*, **5**(10), 2419–2438, (1972). 3.1, 3.5.5

[117] Price, R. H., and Pullin, J., "Colliding black holes: the close limit", *Phys. Rev. Lett.*, **72**(21), 3297–3300, (1994). 3.1, 3.6

[118] Renaut, R., "Absorbing boundary conditions, difference operators, and stability", *J. Comput. Phys.*, **102**(2), 236–251, (1992). 4.1

[119] Rendall, A., "Local and global existence theorems for the Einstein equations", (January, 2000), [Article in Online Journal Living Reviews in Relativity]: cited on 18 January 2001, `http://www.livingreviews.org/Articles/Volume3/2000-1rendall`. 2

[120] Ryaben'kii, V., and Tsynkov, S. V., "An Application of the Difference Potentials Method to Solving External Problems in CFD", in Hafez, M., and Oshima, K., eds., *Computational Fluid Dynamics Review*, volume 2, (World Scientific, Singapore, 1998). 4.1

[121] Sachs, R. K., "Asymptotic symmetries in gravitational theory", *Phys. Rev.*, **128**, 2851–2864, (1962). 3.4

[122] Sachs, R. K., "Gravitational waves in general relativity VIII. Waves in asymptotically flat space-time", *Proc. R. Soc. London, Ser. A*, **270**, 103–126, (1962). 2, 3.3.2

[123] Sachs, R. K., "On the characteristic initial value problem in gravitational theory", *J. Math. Phys.*, **3**(5), 908–914, (1962). 2, 3.6

[124] Scheel, M. A., L., Shapiro S., and Teukolsky, S. A., "Collapse to black holes in Brans-Dicke theory: I. Horizon boundary conditions for dynamical spacetimes", *Phys. Rev. D*, **51**(8), 4208–4235, (1995). 4.4.3

[125] Scheel, M. A., L., Shapiro S., and Teukolsky, S. A., "Collapse to black holes in Brans-Dicke theory: II. Comparison with general relativity", *Phys. Rev. D*, **51**(8), 4236–4249, (1995). 4.4.3

[126] Shapiro, S. L., Teukolsky, S., and Winicour, J., "Toroidal black holes and topological censorship", *Phys. Rev. D*, **52**(12), 6982–6987, (1995). 3.6

[127] Shapiro, S. L., Teukolsky, S. A., and Winicour, J., "Toroidal Black Holes and Topological Censorship", *Phys. Rev. D*, **52**(11), 6982–6987, (1995). 3

[128] Sod, G. A., *Numerical Methods in Fluid Dynamics*, (Cambridge University Press, Cambridge, 1985). 4.1

[129] Sorkin, R., "A criterion for the onset of instability at a turning point", *Astrophys. J.*, **249**(1), 254–257, (1981). 3.1

[130] Sperhake, U., Sjödin, K. R. P., and Vickers, J. A., "Dynamic cosmic strings I", *Phys. Rev. D*, **63**, 024011, (2001). 3.1

[131] Sperhake, U., Sjödin, K. R. P., and Vickers, J. A., "Dynamic cosmic strings II: Numerical evolution of excited strings", *Phys. Rev. D*, **63**, 024012, (2001). 3.1

[132] Stark, R. F., and Piran, T., "A general relativistic code for rotating axisymmetric configurations and gravitational radiation: Numerical methods and tests", *Comput. Phys. Rep.*, **5**(5), 221–264, (1987). 4.5

[133] Stewart, J. M., "Numerical relativity", in Bonnor, W. B., Isham, J. N., and MacCallum, M. A. H., eds., *Classical General Relativity*, 231, (Cambridge University Press, Cambridge, 1984). 3.1

[134] Stewart, J. M., "The characteristic initial value problem in general relativity", in Winkler, K.-H. A., and Norman, M. L., eds., *Astrophysical Radiation Hydrodynamics*, 531, (Reidel, Dordrecht, 1986). 3

[135] Stewart, J. M., "Numerical relativity III. The Bondi mass revisited", *Proc. R. Soc. London, Ser. A*, **424**, 211–222, (1989). 3.3.1, 3.4

[136] Stewart, J. M., and Friedrich, H., "Numerical relativity I. The characteristic initial value problem", *Proc. R. Soc. London, Ser. A*, **384**, 427–454, (1982). 1, 3.3.1

[137] Szilágyi, B., *Cauchy-characteristic matching in general relativity*, PhD Thesis, (University of Pittsburgh, Pittsburgh, USA, 2000). 1, 4

[138] Szilágyi, B., Gómez, R., Bishop, N. T., and Winicour, J., "Cauchy boundaries in linearized gravitational theory", *Phys. Rev. D*, **62**, 104006, (2000). 3.5.3, 4

[139] Tamburino, L. A., and Winicour, J., "Gravitational Fields in Finite and Conformal Bondi Frames", *Phys. Rev.*, **150**(4), 1039–1053, (1966). 2, 3.4, 5

[140] Teukolsky, S. A., "Linearized quadrupole waves in general relativity and the motion of test particles", *Phys. Rev. D*, **26**(4), 745–750, (1982). 3.3

[141] The Binary Black Hole Grand Challenge Alliance, "Boosted three-dimensional black hole evolution with singularity excision", *Phys. Rev. Lett.*, **80**(12), 2512–2516, (1998). 3.3, 4.7

[142] The Binary Black Hole Grand Challenge Alliance, "Gravitational wave extraction and outer boundary conditions by perturbative matching", *Phys. Rev. Lett.*, **80**(9), 1812–1815, (1998). 1, 4.3

[143] The Binary Black Hole Grand Challenge Alliance, "Stable characteristic evolution of generic 3-dimensional single-black-hole spacetimes", *Phys. Rev. Lett.*, **80**(18), 3915–3918, (1998). 3.5.3

[144] Thompson, K. W., "Time=dependent boundary conditions for hyperbolic systems", *J. Comput. Phys.*, **68**, 1–24, (1987). 4.1

[145] Thornburg, J., "Coordinates and boundary conditions for the general relativistic initial data problem", *Class. Quantum Grav.*, **4**(5), 1119–1139, (1987). 4.1

[146] Ting, L., and Miksis, M., "Exact boundary conditions for scattering problems", *J. Acoust. Soc. Am.*, **80**(6), 1825–1827, (1986). 4.1

[147] Trefethen, L., and Halpern, L., "Well-posedness of one-way wave equations and absorbing boundary conditions", *Math. Comput.*, **47**, 421–435, (1986). 4.1

[148] Tsynkov, S. V., *Artificial Boundary Conditions Based on the Difference Potentials Method*, (NASA, 1996), Report no. 110265. NASA Technical Memorandum. 4.1

[149] University of Canberra, "Home Page", [Online HTML Document]: cited on 18 January 2001, `http://gular.canberra.edu.au/relativity.html`. 1

[150] University of Pittsburgh, "Home Page", [Online HTML Document]: cited on 18 January 2001, `http://julieta.phyast.pitt.edu/~wwwgr/`. 1, 3.6

[151] Wald, R. M., *General Relativity*, (University of Chicago Press, Chicago, 1984). 4.4.3

[152] Weber, J., and Wheeler, J. A., "Reality of the cylindrical gravitational waves of Einstein and Rosen", *Proc. R. Soc. London, Ser. A*, **29**, 509, (1957). 3.1, 4.4.1

[153] Winicour, J., "The Quadrupole Radiation Formula", *Gen. Relativ. Gravit.*, **19**(3), 281–287, (1987). 4.2

[154] Winicour, J., "The Characeristic Traetment of Black Holes", *Prog. Theor. Phys. Suppl.*, **136**, 57–71, (1999). 3.6, 3.6

[155] Xanthopoulos, B. C., "Cylindrical waves and cosmic strings of Petrov type D", *Phys. Rev. D*, **34**(12), 3608–3616, (1986). 3.1

[156] York, J., "Kinematics and dynamics of general relativity", in Smarr, L. L., ed., *Sources of Gravitational Radiation*, 83–126, (Cambridge University Press, Cambridge, 1979). 1

[157] Zum Hagen, M., and Seifert, H., "On characteristic initial value and mixed problems", *Gen. Relativ. Gravit.*, **8**(4), 259–301, (1977). 3.6